Constraints on Primordial Magnetic Fields with Faraday Rotation. Impact of CMB foregrounds

J.A. Rubiño- Martín (IAC)

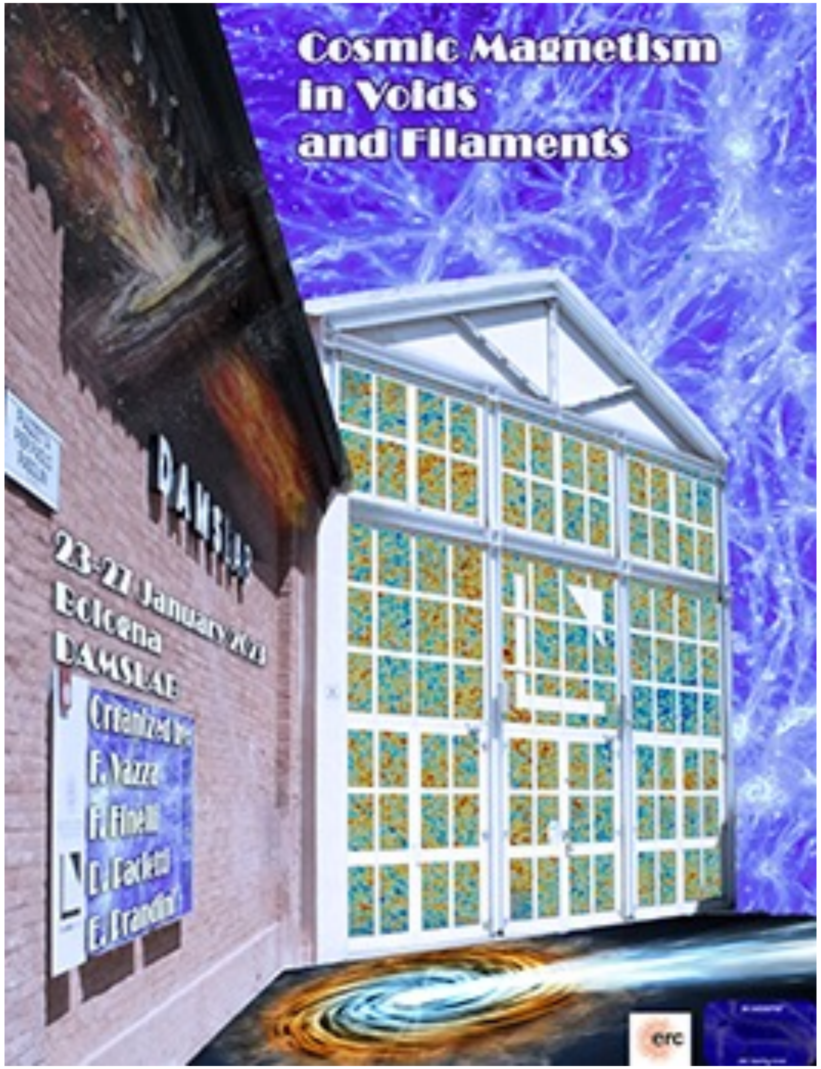

Outline:

I. Faraday Rotation and Primordial Magnetic Fields
   i. Overview of the theory.
   ii. Current constraints.

II. Impact of CMB foregrounds.
   i. Galactic FR
   ii. Synchrotron emission: status of current measurements.

25 January 2023

Faraday Rotation (FR)

It is a propagation effect in a **magnetised cold plasma**. A plane polarized wave will rotate its polarization plane as it propagates, due to the different velocities of R and L waves.

In gaussian cgs units (e.g. Rybicki & Lightman):

$$\epsilon_{R,L} = 1 - \frac{\omega_p^2}{\omega(\omega \pm \omega_B)}$$

$$\Delta\theta = \frac{1}{2}\int_0^d \frac{\omega_p^2 \omega_B}{c\omega^2} ds = \frac{2\pi e^3}{m^2 c^2 \omega^2}\int_0^d n_e B_{\parallel} ds$$

$$\Delta\theta = \left(\frac{e^3}{2\pi m^2 c^4}\int_0^d n_e B_{\parallel} ds\right)\lambda^2 = RM\lambda^2$$

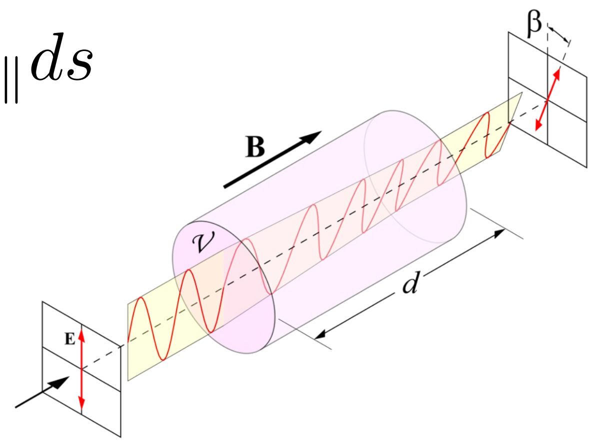

where RM stands for **Rotation Measure**, which depends on the axial component of the magnetic field and the (thermal) electron number density.

We usually use the concept of **Faraday depth** (Burn 1966; Brentjens & De Bruyn 2005):

$$\phi(\vec{r}) = K \int n_e(r) B_{\parallel}(r) d\vec{r}$$

, $K=0.81$ rad m^{-2} pc^{-1} cm^3 μG^{-1}

Primordial Magnetic Fields (PMF) and FR

If there were a PMF at the recombination epoch, or after the Universe was reionized, it would induce FR on the CMB photons, mixing Q and U Stokes parameters.

RMS rotation angle can be easily estimated, noting that B/ν^2 is time independent (see Kosowsky & Loeb 1996, Harari et al. 1997):

$$\langle\varphi^2\rangle^{1/2} \approx \frac{e^3 B_0}{2\sqrt{2\pi m^2 \sigma_T \nu_0^2}} = 1\overset{\circ}{.}6 \left(\frac{B_0}{10^{-9}\ \mathrm{G}}\right)\left(\frac{30\ \mathrm{GHz}}{\nu_0}\right)^2$$

where they used that the optical depth for Thomson scattering is of the order of unity out to the redshift of decoupling.

$$\int x_e n_e dt \approx 1/\sigma_T$$

PMF and FR (II)

Effect on CMB polarization anisotropies (Kosowsky & Loeb 1996): mixing terms between Q and U components along the propagation. In comoving coordinates:

$$\begin{aligned}
\dot{\Delta}_I + ik\mu(\Delta_I - 4\Phi) &= -4\dot{\Psi} \\
&\quad - \dot{\tau}[\Delta_I - \Delta_{I0} + 4v_b\mu - \tfrac{1}{2}P_2(\mu)(\Delta_{I2} + \Delta_{Q2} - \Delta_{Q0})] , \\
\dot{\Delta}_Q + ik\mu\Delta_Q &= -\dot{\tau}\{\Delta_Q + \tfrac{1}{2}[1 - P_2(\mu)] \\
&\quad \times (\Delta_{I2} + \Delta_{Q2} - \Delta_{Q0})\} + 2\omega_{\boldsymbol{B}}\Delta_U , \\
\dot{\Delta}_U + ik\mu\Delta_U &= -\dot{\tau}\,\Delta_U - 2\omega_{\boldsymbol{B}}\Delta_Q \qquad (3)
\end{aligned}$$

* No magnetically induced perturbations

Where w_B represents the conformal FR rate:

$$\omega_{\boldsymbol{B}} \equiv \frac{d\varphi}{d\eta} = \frac{d\varphi}{dt}\,\frac{a}{a_0} \qquad\qquad \frac{d\varphi}{dt} = \frac{e^3 x_e n_e}{2\pi m^2 \nu^2}(\boldsymbol{B}\cdot\hat{\boldsymbol{q}})$$

At the power spectrum level, FR generates a B-mode signal which is frequency dependent. Two cases have been studied in the literature: **homogeneous PMF** (see, e.g., Scóccola et al. 2004) or **stochastic PMF** (see, e.g., Kosowsky et al. 2005).

PMF and FR: homogeneous PMF

Homogeneous PMF:

$$F = \frac{3}{8\pi^2}\frac{Bc^2}{\nu^2 e} \approx 0.7\left(\frac{B}{10^{-9}\ \mathrm{G}}\right)\left(\frac{10\ \mathrm{GHz}}{\nu}\right)^2$$

A B-mode component is generated from the initial E-mode, which correlates with T and E.

BB autocorrelation scaling as F^2. Strong frequency dependence!

TB correlations are non diagonal (between different ell), with strength scaling as F.

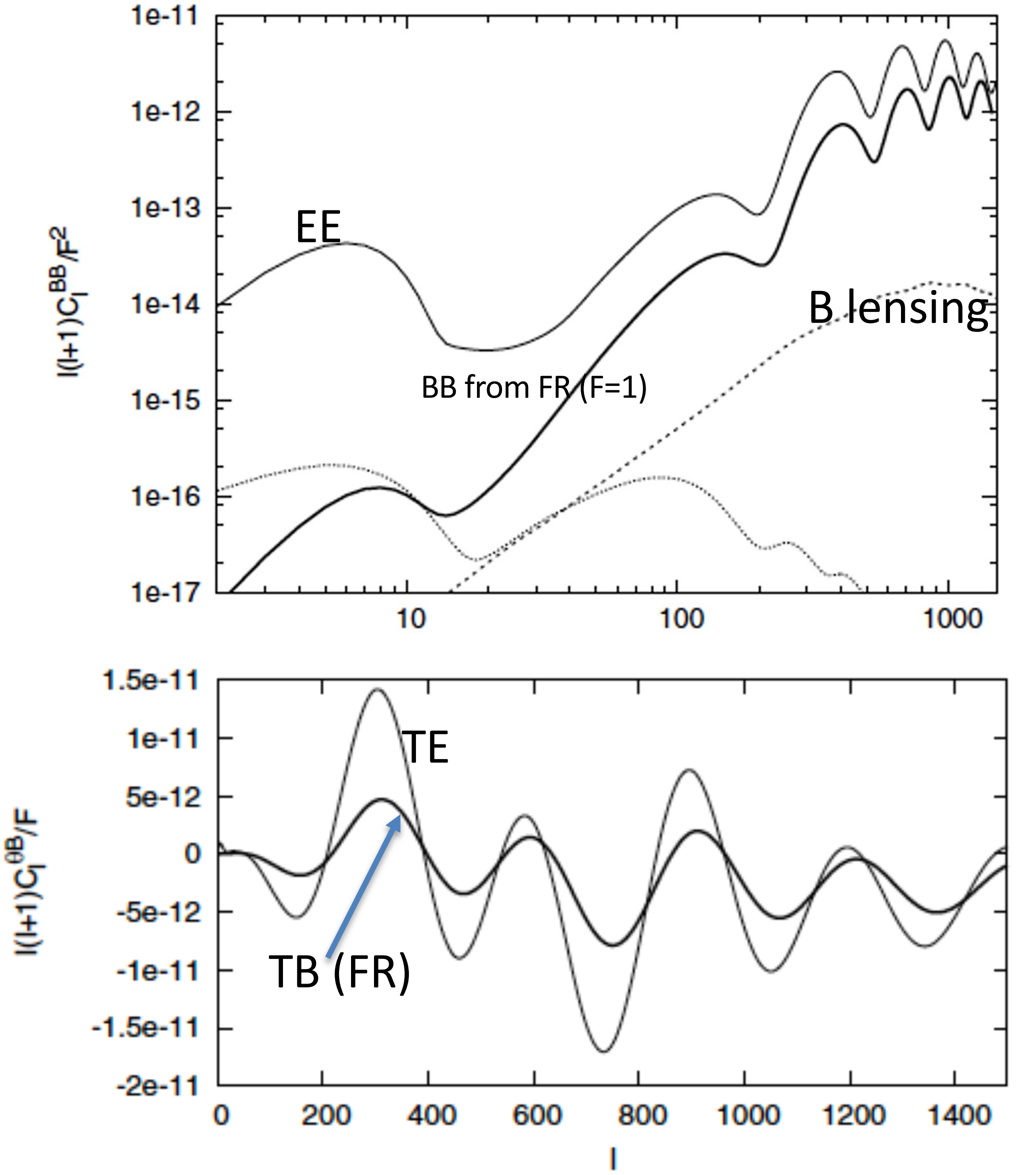

Scoccola et al. (2004)

PMF and FR: stochastic PMF

- **References:** Kosowsky et al. 2005, Kahniashvili et al. 2009; Guan & Kosowsky 2022. See also Pogosian et al. 2011.
- Helical part of the field does not contribute to the FR (Campanelli et al. 2004).

$$\left\langle B_i(k)\, B_j^*(k')\right\rangle = \frac{(2\pi)^3}{2}\,\delta^{(3)}(k-k')\left(\delta_{ij}-\hat{k}_i\hat{k}_j\right) P_B(k) \qquad P_{\rm B}(k) = A_{\rm B} k^{n_{\rm B}}$$

- Field smoothed on a given Gaussian scale:

$$B_\lambda^2 \quad = \quad \int_0^\infty \frac{{\rm d}k\, k^2}{2\pi^2}\, {\rm e}^{-k^2\lambda^2} P_B(k) = \frac{A_B}{4\pi^2\lambda^{n_B+3}}\,\Gamma\left(\frac{n_B+3}{2}\right).$$

- Magnetic field cutoff scale is determined by the Alfven wave damping scale.

$$\left(\frac{k_D}{{\rm Mpc}^{-1}}\right)^{n_B+5} \approx 2.9\times10^4\left(\frac{B_\lambda}{10^{-9}\ {\rm G}}\right)^{-2}\left(\frac{k_\lambda}{{\rm Mpc}^{-1}}\right)^{n_B+3} h,$$

- **Rotation power spectrum.**

$$\alpha(\mathbf{n},\eta_0) = \frac{3}{(4\pi)^2\nu_0^2 q}\int_{\eta_{\rm dec}}^{\eta_0} d\eta\,\dot{\tau}(\eta)\mathbf{B}(\mathbf{x})\cdot\mathbf{n}. \qquad R(\mathbf{n}) \equiv \alpha(\mathbf{n})\nu_0^2.$$

$$C_l^R \simeq \frac{9l(l+1)}{(4\pi)^3 q^2}\,\frac{B_\lambda^2}{\Gamma(n_B/2+3/2)}\left(\frac{\lambda}{\eta_0}\right)^{n_B+3}\int_0^{x_D} dx\, x^{n_B} j_l^2(x)$$

PMF and FR: stochastic PMF

Rotation power spectrum.

$$C_l^R \simeq \frac{9l(l+1)}{(4\pi)^3 q^2} \frac{B_\lambda^2}{\Gamma(n_B/2+3/2)} \left(\frac{\lambda}{\eta_0}\right)^{n_B+3} \int_0^{x_D} dx x^{n_B} j_l^2(x)$$

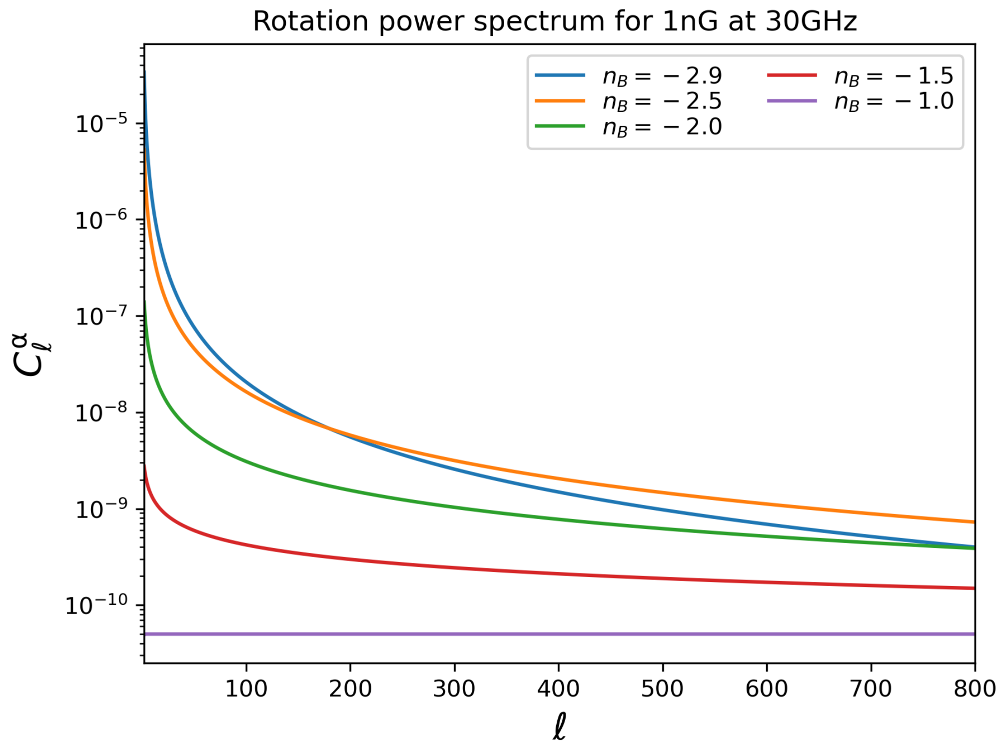

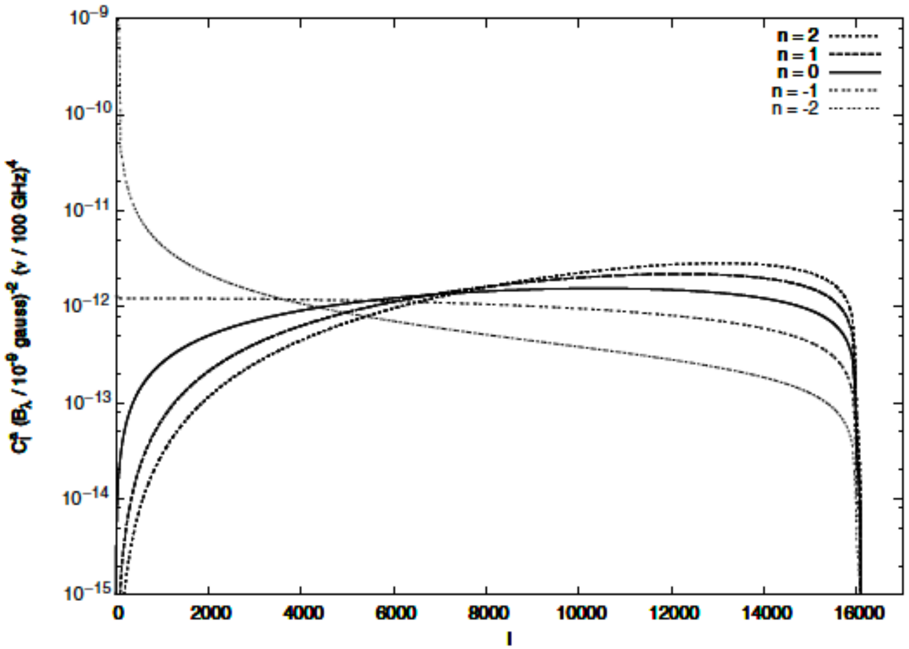

Kosowsky et al. (2005)

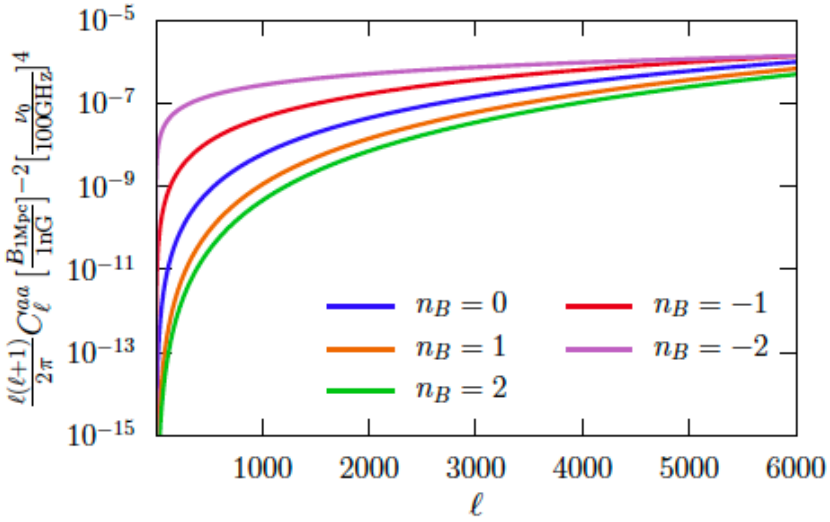

Guan & Kosowsky (2022)

PMF and FR: stochastic PMF

Refs: Kosowsky et al. 2005; Pogosian et al 2011; Guan & Kosowsky 2022.

Effectively, we have **B-mode generation**. The BB polarization induced spectrum by the primordial E mode is (in the thin last-scattering surface approximation):

$$C_\ell^{\prime BB} = N_\ell^2 \sum_{\ell_1 \ell_2} \frac{(2\ell_1+1)(2\ell_2+1)}{4\pi(2\ell+1)} \times N_{\ell_2}^2 K(\ell,\ell_1,\ell_2)^2 C_{\ell_2}^{EE} C_{\ell_1}^{\alpha} \left(C_{\ell_1 0 \ell_2 0}^{\ell 0}\right)^2$$

Exact computation (thick LSS) in Pogosian et al. 2011.

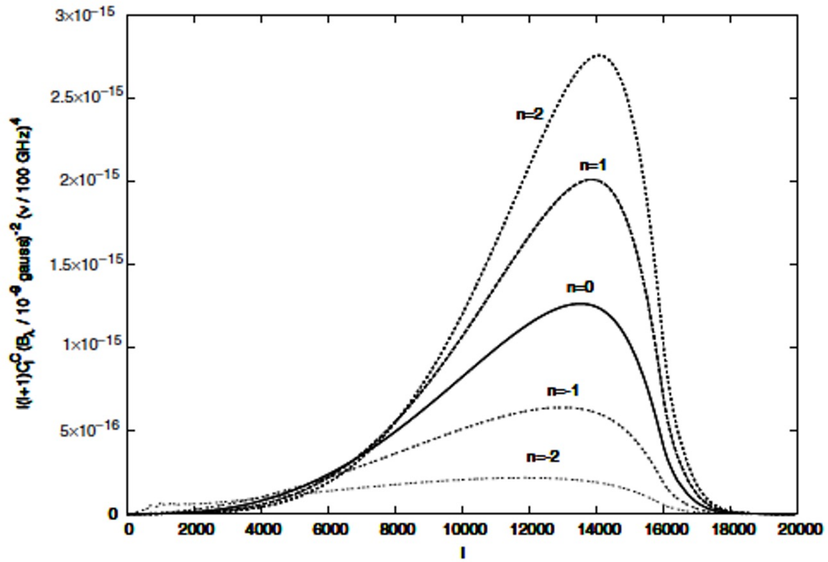

FIG. 2. The C-polarization power spectrum of the microwave background induced by the Faraday rotation field in Fig. 1, again with the magnetic field normalization scale $\lambda = 1$ Mpc.

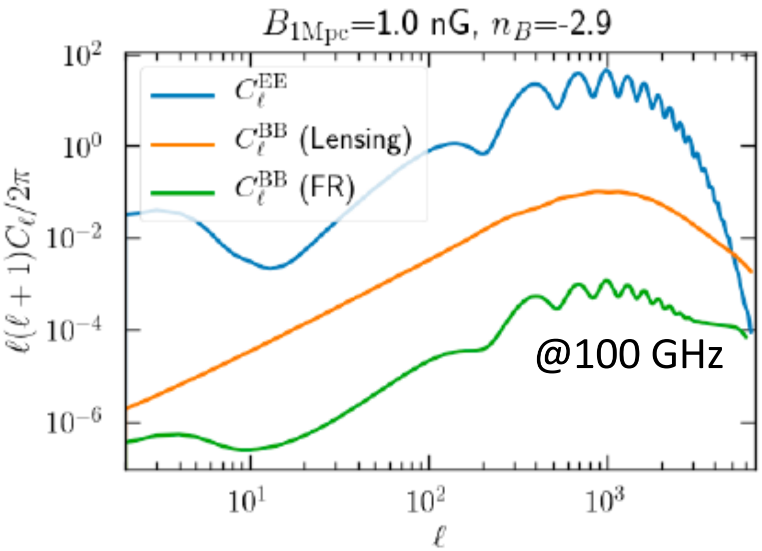

Existing constraints on FR - pre Planck

WMAP data. Analysis is carried out at a given frequency.
Combined results Q, V, W bands. Multipoles l>32.

WMAP-5: Kahniashvili et al. (2009). WMAP-7 (Pogosian et al. 2011).

B< 100nG, and suggest n_B ~-2.9.

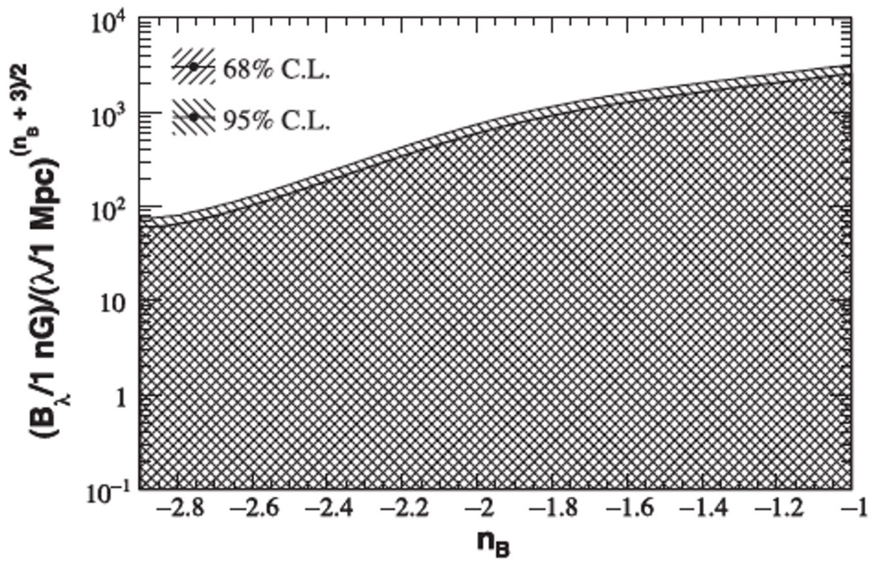

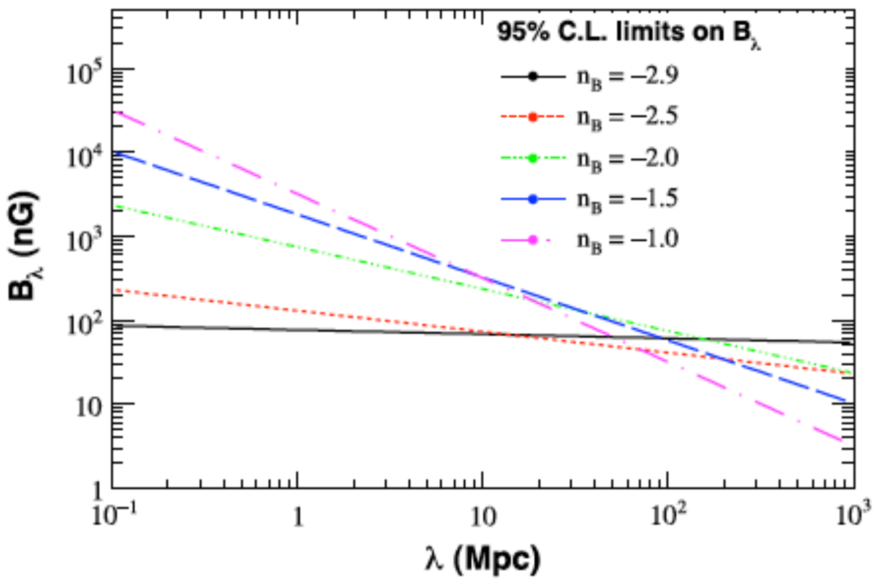

Existing constraints on FR – Planck and future CMB exp.

Planck 2015 results XIX (PC 2016)

Analysis based on LFI70 only!

$B_{1\,\mathrm{Mpc}}$ < (1040; 1380) nG (68%, 95% CL)

Spectral index remains unconstrained.

Upper bounds are high compared to other methods. But totally independent, and make use of an unique feature to identify PMFs.

→ Room for improvement: full Planck likelihood.

→ Forecasts for future CMB experiments (Litebird, SO, CMB-S4).

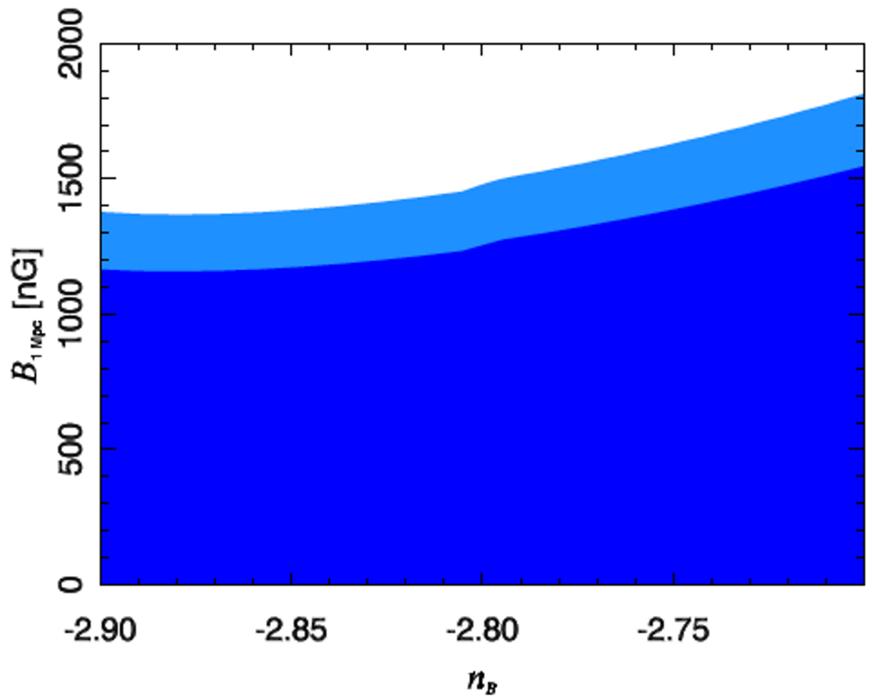

Fig. 12. Probability contours of PMF strength vs. spectral index of the PMF power spectrum as constrained by the 70 GHz observations.

Stochastic PMF and rotation angle

Root-mean-square rotation angle

Accounting for the beam (no depol), we have:

$$< \alpha^2 >^{1/2} = \left[\sum_\ell \frac{2\ell + 1}{4\pi} C_\ell^\alpha W_\ell \right]^{1/2}$$

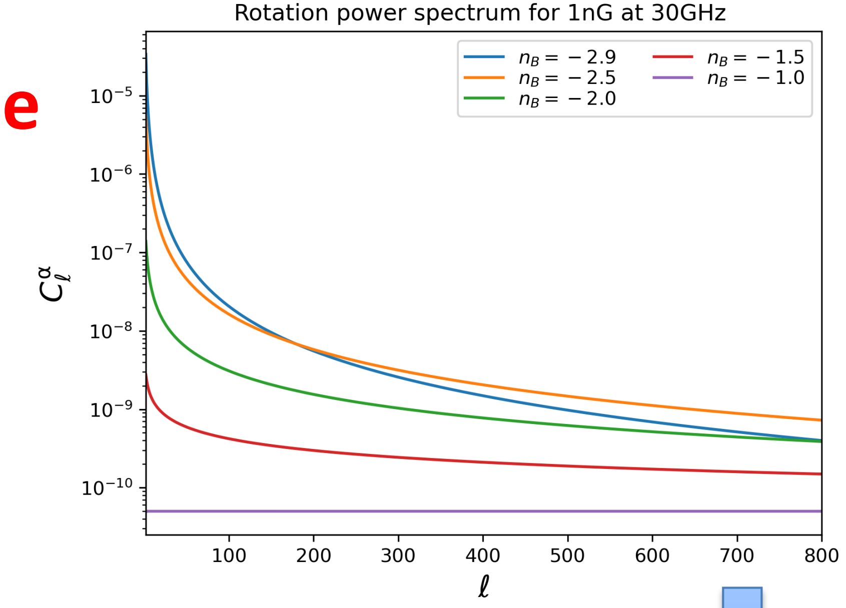

For Litebird-like experiment (FWHM~30') we have about 0.7deg rms for 1nG scale-invariant PMF at 30GHz. But strong dependence on n_B!

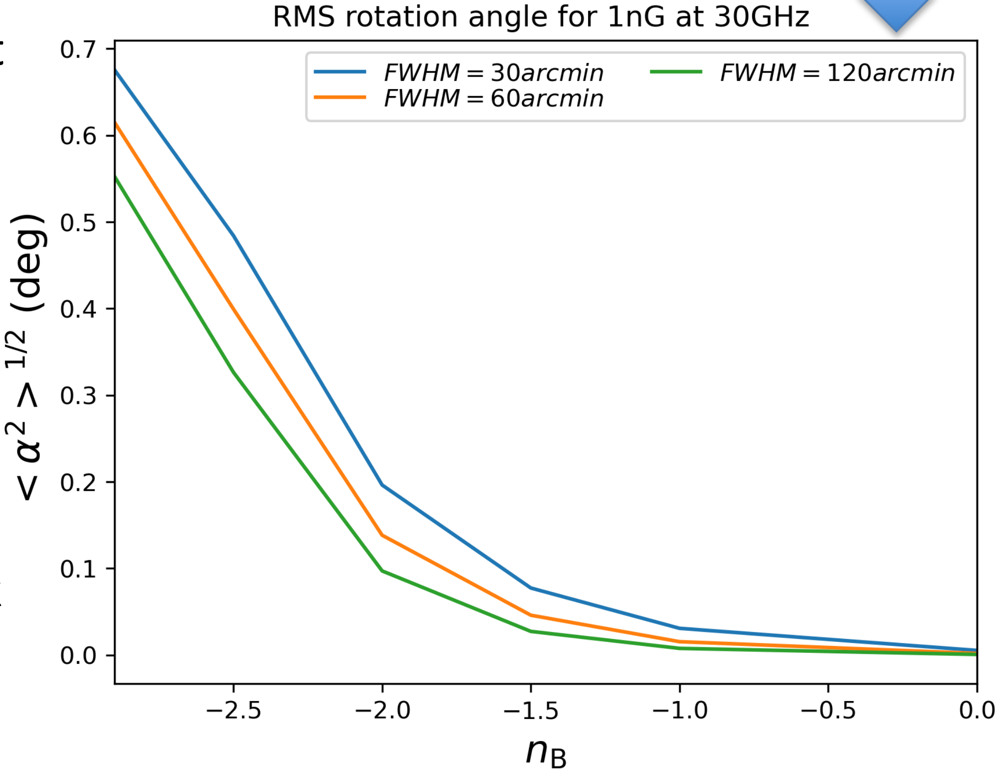

Consistent with SI case in De et al. (2013):

$$B_{\rm eff} \approx 0.021\ A_{\rm RM}\ \frac{\rm nG\ m^2}{\rm rad}$$

Used to convert **anisotropic birefringence limits** into PMF (see Grupusso et al. 2018, talk on Thursday). Uses TB,EB,BB. Limits ~26nG.

Constraints on Primordial Magnetic Fields with Faraday Rotation. Impact of CMB foregrounds

J.A. Rubiño- Martín (IAC)

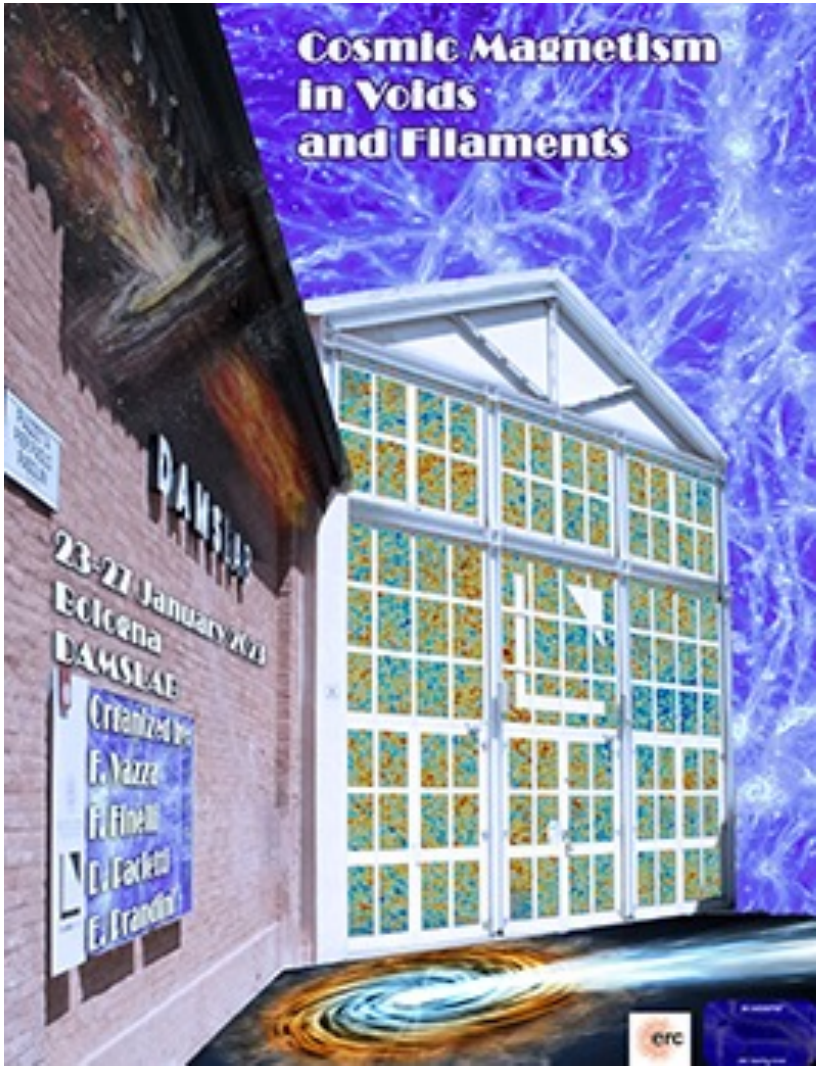

Outline:

I. Faraday Rotation and Primordial Magnetic Fields
   i. Overview of the theory.
   ii. Current constraints.

II. Impact of CMB foregrounds.
   i. Galactic FR
   ii. Synchrotron emission: status of current measurements.

Galactic contamination level (Faraday depth)

Estimated using:

- Observations of the polarized synchrotron emission at 1.4 GHz (Wolleben et al. 2006) and 23 GHz (WMAP-K).
- Synthesized all-sky Faraday rotation map derived from extragalactic radio source emission (Oppermann et al. 2015).

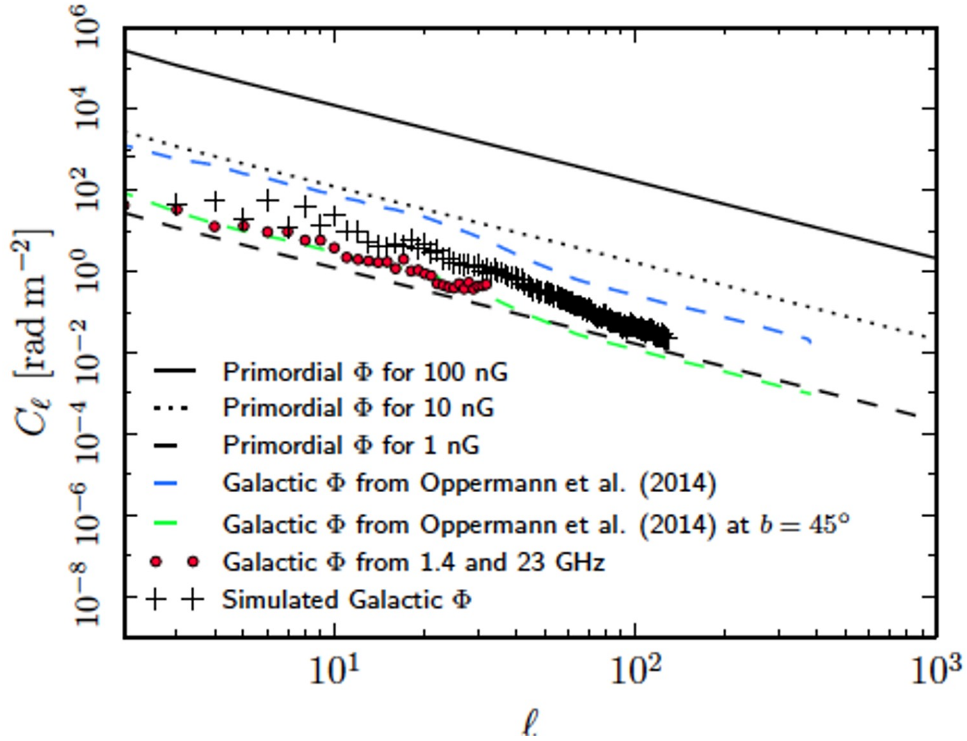

Expected contamination levels below 10nG for full sky.

Planck Collaboration XIX 2016

Galactic Faraday depth

Oppermann et al. 2015

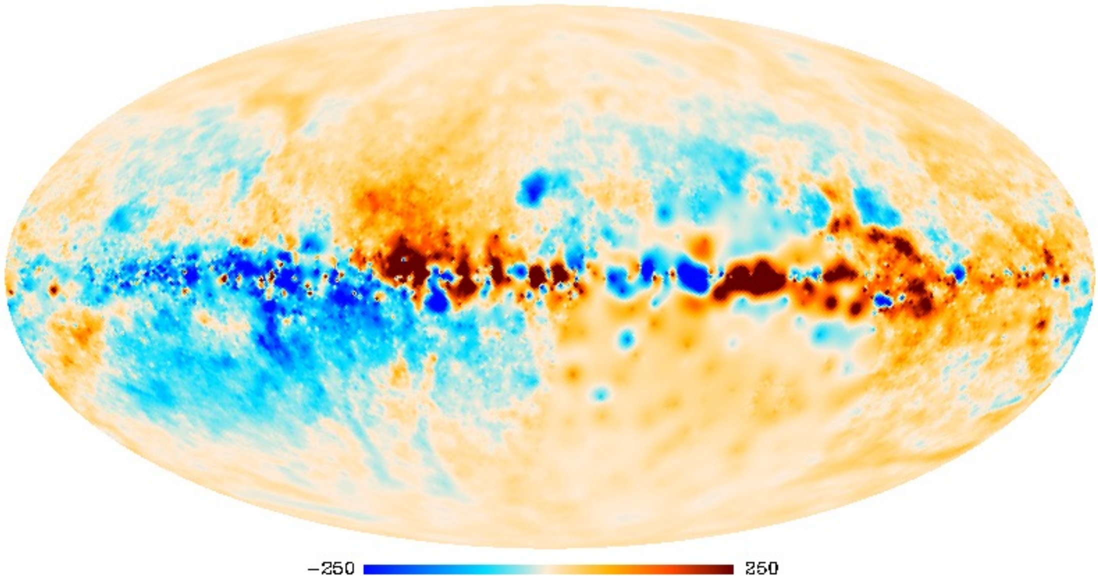

Hutschenreuter et al. 2020

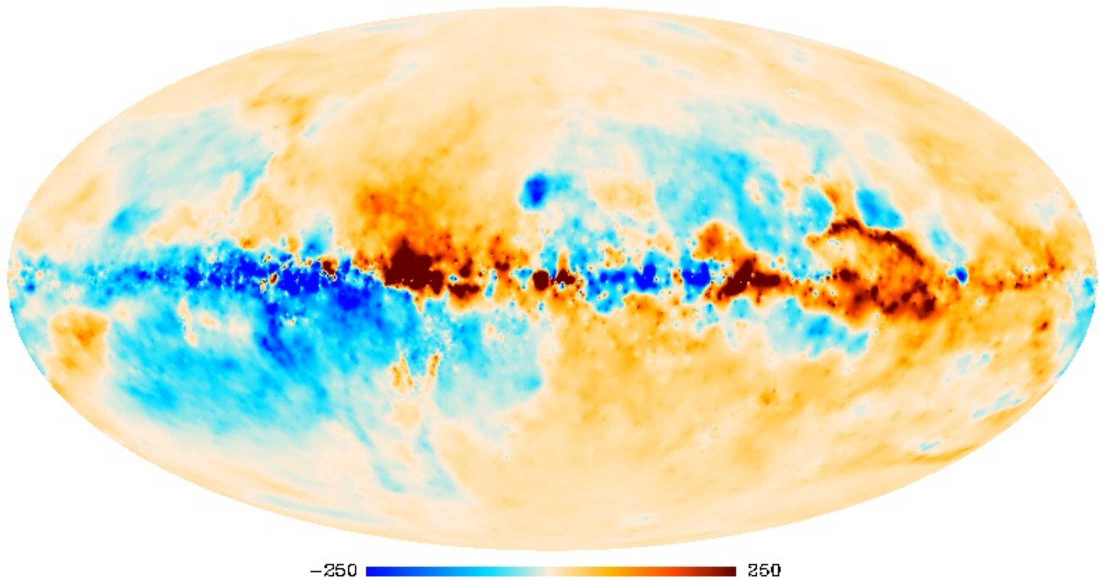

Galactic contamination level (Faraday depth)

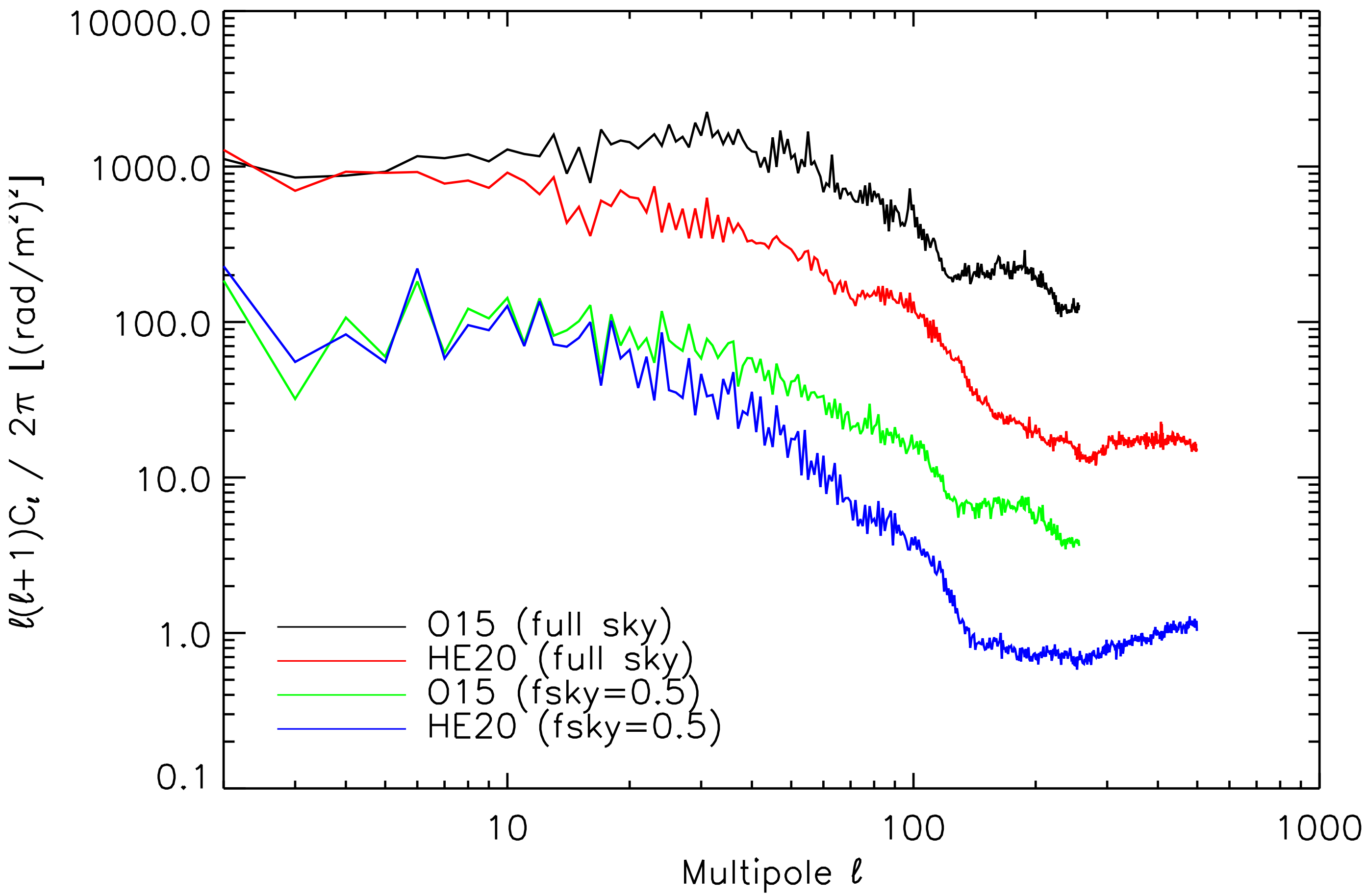

Expected contamination levels in partial sky (|b|<30º) decreased by factor 10, to values 10 rad/m^2 at large scales.

Consistent with the estimates of Pogosian 2013; De et al. 2013.

Synchrotron with low frequency data

Component separation problem for extracting the polarised CMB signal at a given frequency channel. Primordial signal subdominant. FR of the Galactic emission not treated yet.

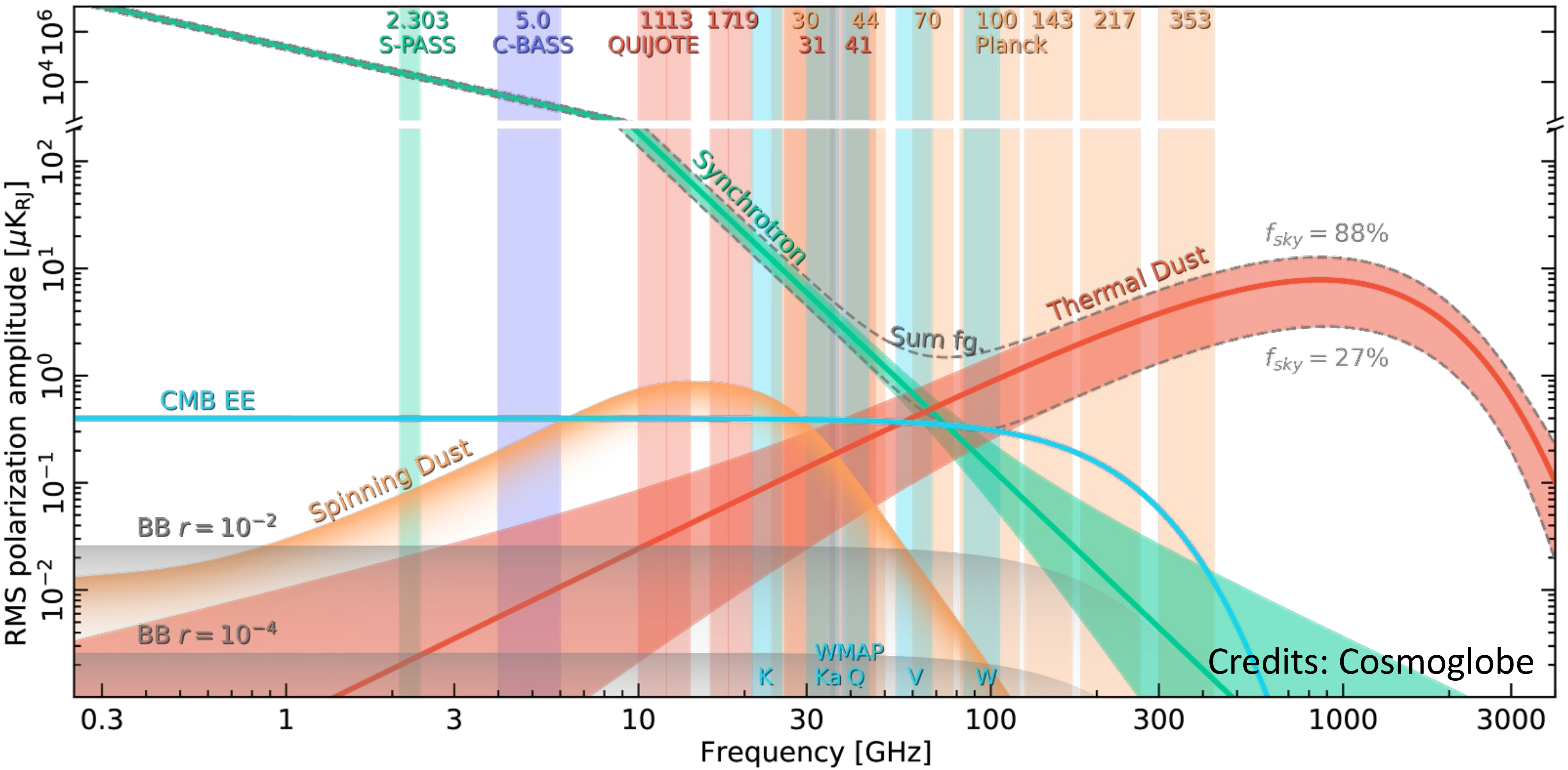

New surveys at low frequencies! See "Galactic Science & CMB foregrounds", Tenerife, December 12-15, 2022. https://www.astr.tohoku.ac.jp/GSWS/program.html

Synchrotron with low frequency data

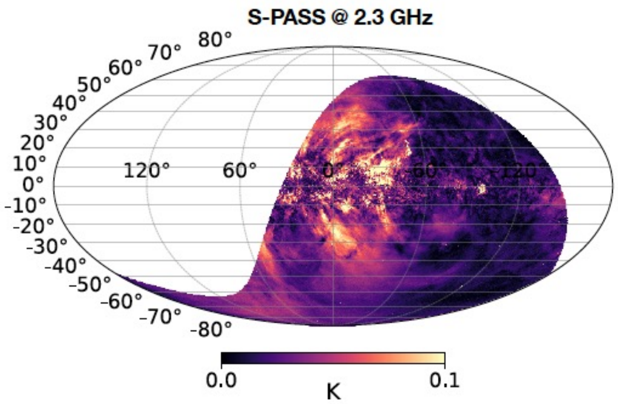

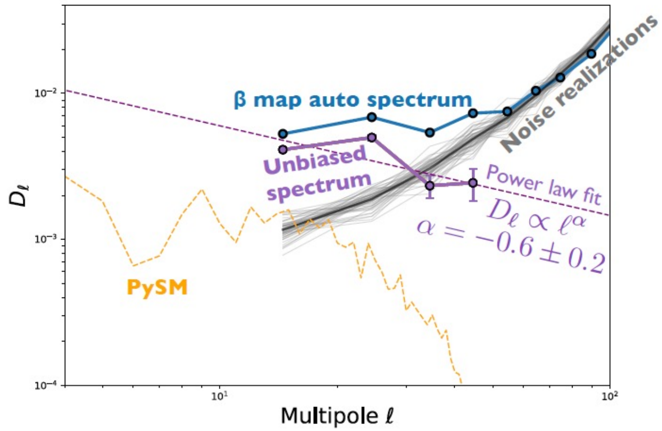

From N. Krachmalnicoff presentation.
→ See talk on Thursday by C. Baccigalupi

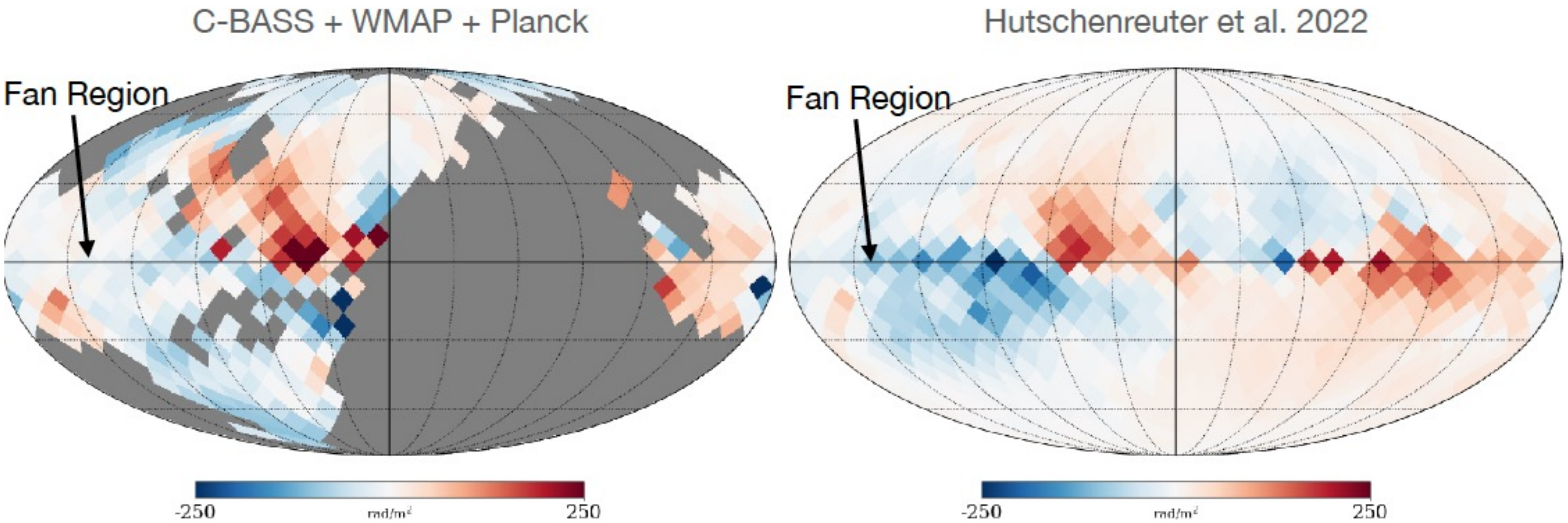

(From S. Harper presentation)

The QUIJOTE experiment

Quijote
Q-U-I Joint Tenerife CMB experiment

RADIO FOREGROUNDS

QT-1 and QT-2: Crossed-Dragone telescopes, 2.25m primary, 1.9m secondary.

QT-1. Instruments: MFI, MFI2.
11, 13, 17, 19 GHz.
FWHM=0.93º-0.62º
MFI: 2012-18.
MFI2: 2023-

QT-2. Instruments: TGI & FGI
30 and 40 GHz.
FWHM=0.37º-0.28º
Commissioning 2018.
Observations re-started 2021.

GOBIERNO DE ESPAÑA
MINISTERIO DE CIENCIA E INNOVACIÓN
UNIÓN EUROPEA
Fondo Europeo de Desarrollo Regional
"Una manera de hacer Europa"
Ref. de la ayuda: ICTS-2019-03-IAC-12

INSTITUTO DE ASTROFISICA DE CANARIAS · IAC
IFCA Instituto de Física de Cantabria
DICOM
UNIVERSITY OF CAMBRIDGE
MANCHESTER 1824 The University of Manchester
idom

Wide survey with the QUIJOTE MFI (10-20 GHz)

Smoothed 1 deg maps

(Rubino-Martin et al. 2023)

(Data release Jan 12th 2023: https://research.iac.es/proyecto/quijote. Six papers)

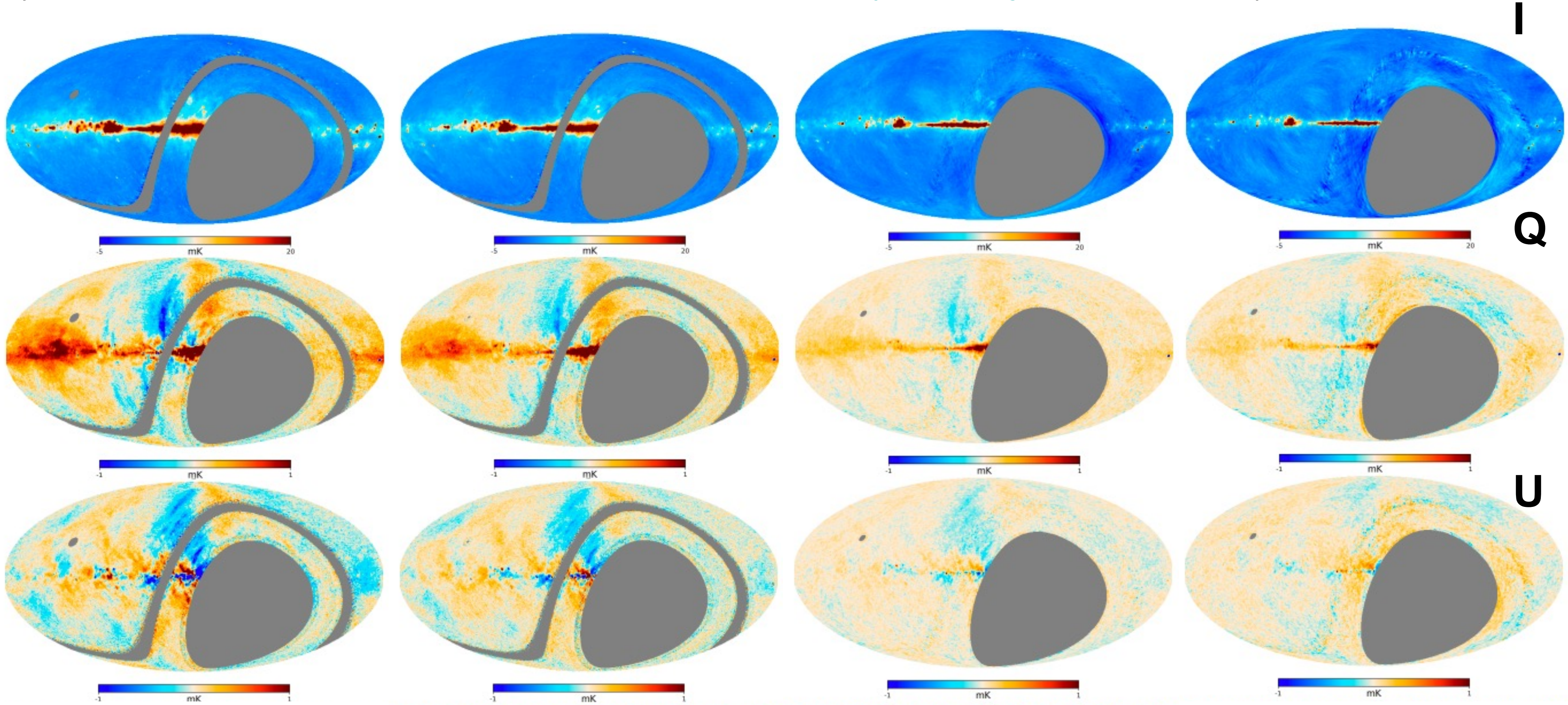

QUIJOTE 11GHz **QUIJOTE 13GHz** **QUIJOTE 17GHz** **QUIJOTE 19GHz**

Approx. 29,000 deg^2. About 10,000 h of observations. Sensitivities in polarization (Q,U): ~35-40 μK/deg → equivalent to 2.4 μK.arcmin @ 100GHz with β=-3.

Wide survey with the QUIJOTE MFI (10-20 GHz)

11GHz **13GHz** **23GHz**

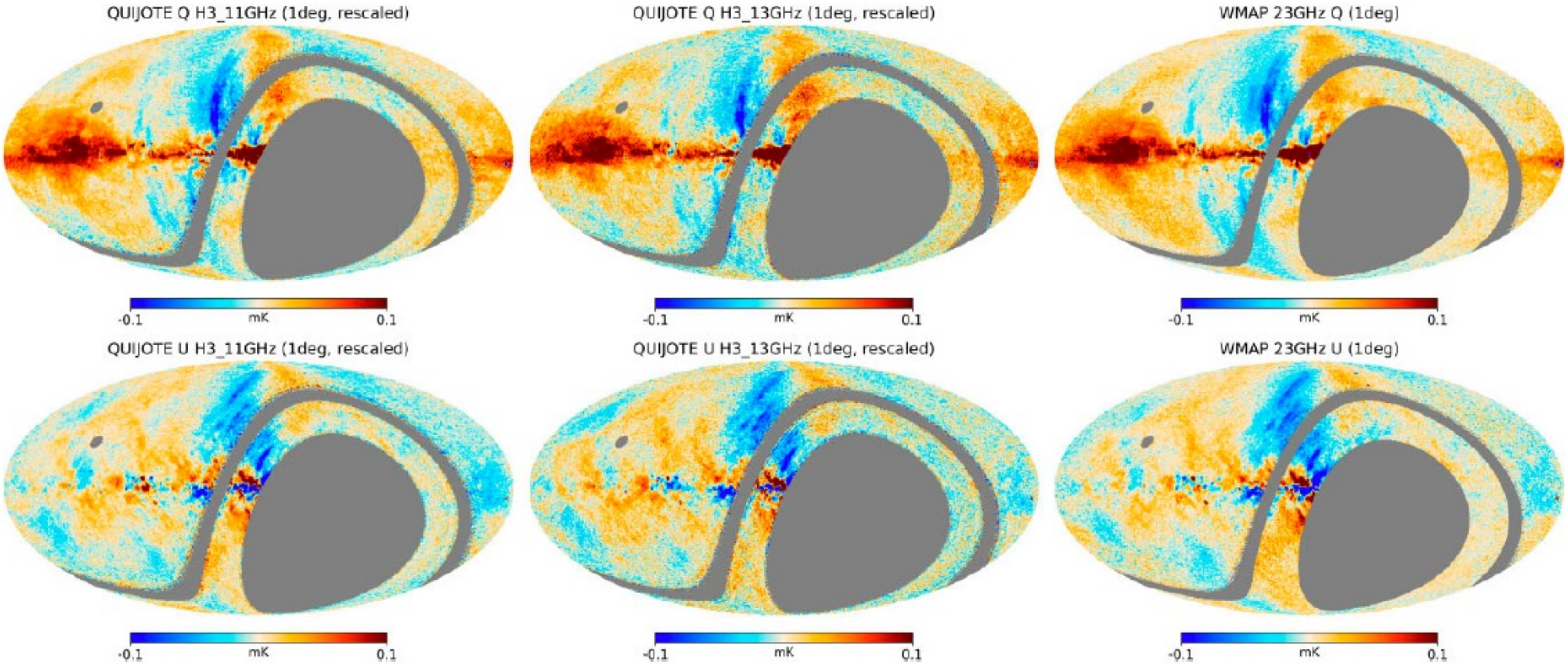

QUIJOTE maps scaled to 23 GHz using β=-3.1. Same colour scale in all maps!
For visualization purposes, the QUIJOTE mask is applied to WMAP 23GHz

(Rubino-Martin et al. 2023)

Wide survey with the QUIJOTE MFI (10-20GHz)

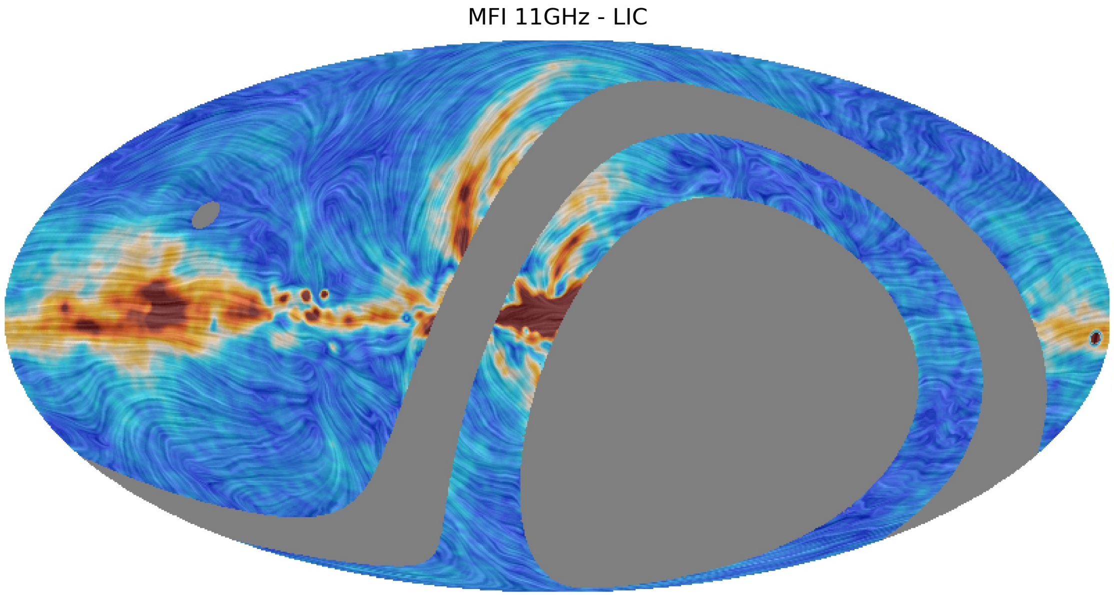

$$P = \sqrt{Q^2 + U^2}$$

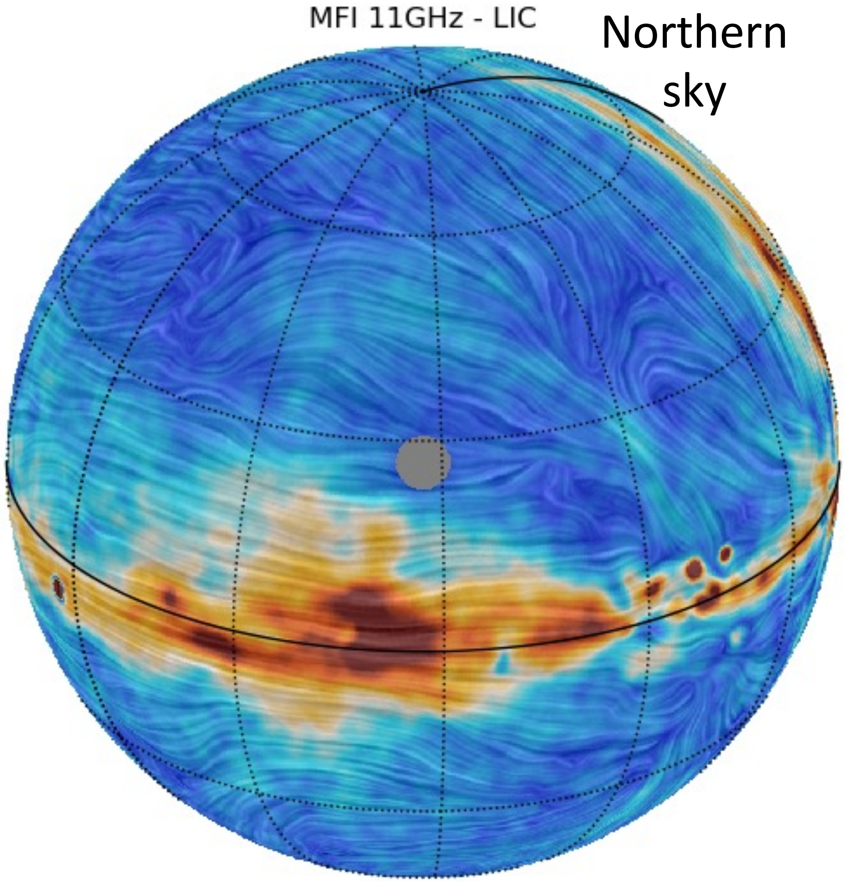

Angles: Comparison to WMAP and PLANCK in high SNR regions, excluding calibrators (CRAB) and high FR regions (galactic center). E.g. the median difference MFI11GHz - LFI30: -0.5º (error=0.6º).

Magnetic fields lines
(Rubino-Martin et al. 2023)

QUIJOTE-MFI wide survey results: synchrotron polarization

Spectral index

$$T \propto \nu^{\beta_S}$$

Spectral index of the polarized synchrotron in the northern sky (de la Hoz et al. 2023). QUIJOTE+WMAP+Planck. Maps at 2 deg and nside=64, and prior N(-3.1,0.3):

$$\boldsymbol{\beta_S = -3.08 \pm 0.13}$$

Significantly broader than existing models! As anticipated by SPASS. PySM synch model 1.

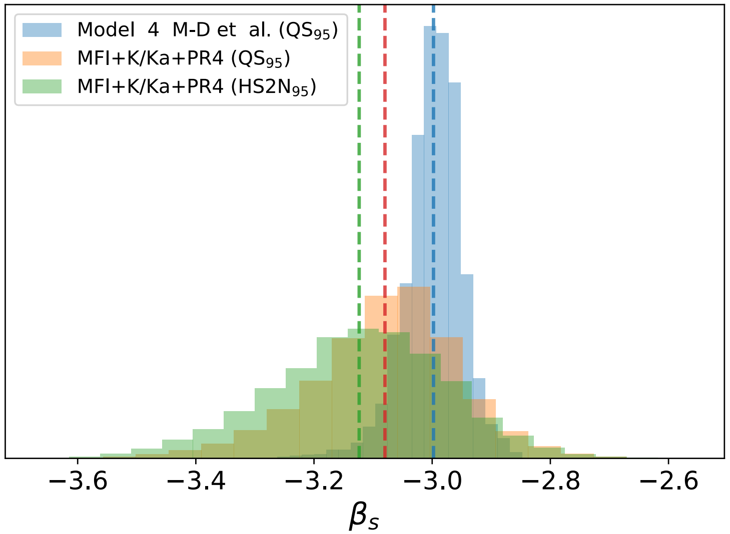

Direct spectral index of QUIJOTE 11GHz and WMAP 23 GHz gives similar result (Rubiño-Martin et al. 2023): **β(11-23GHz) = -3.09 ± 0.14.**

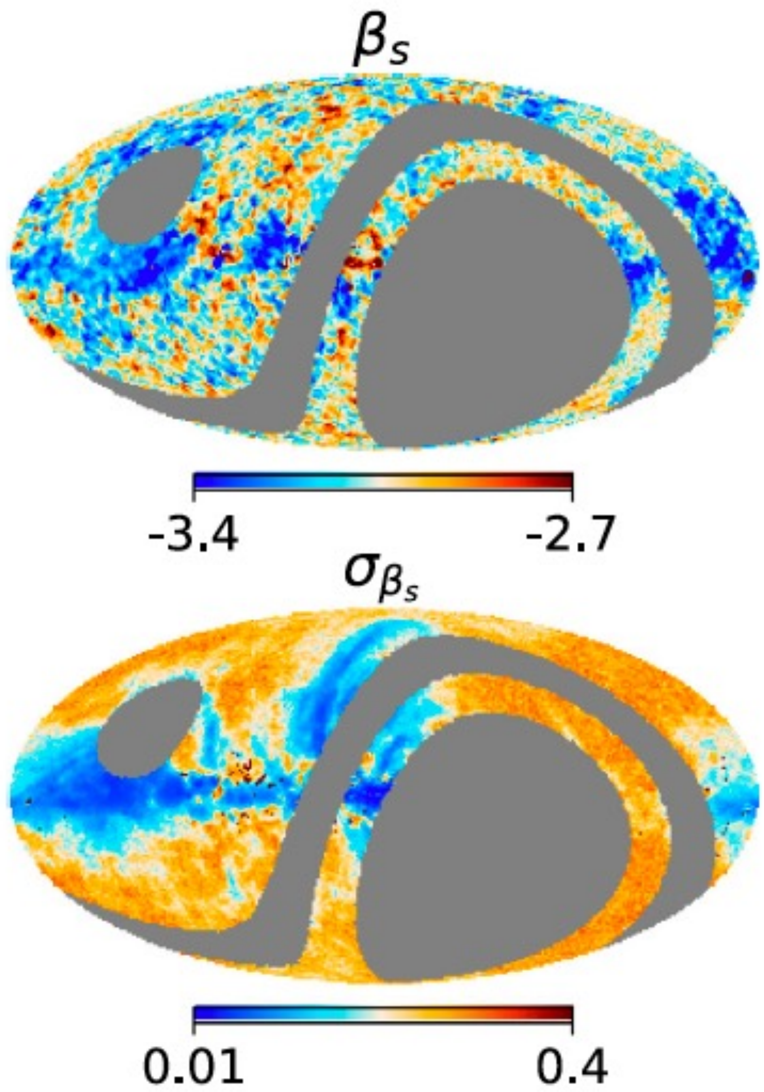

(de la Hoz et al. 2023)

Wide survey with the QUIJOTE MFI (10-20GHz)

Synchrotron E-B modes and E/B ratio

- Most prominent polarized structures (Fan, NPS, loops) appear in the E-map.
- **EE/BB ratio is approx. 4 at large scales**. Consistent with Martire et al. 2022 (WMAP+Planck).
- Analysis at power spectrum level confirms this result (Vansyngel et al. in prep.)
- For thermal dust, the ratio was closer to 2 (BB/EE~0.5, Planck Collaboration XI 2018).
- We measure **EB and TB consistent with zero**. Positive TE at large angular scales.

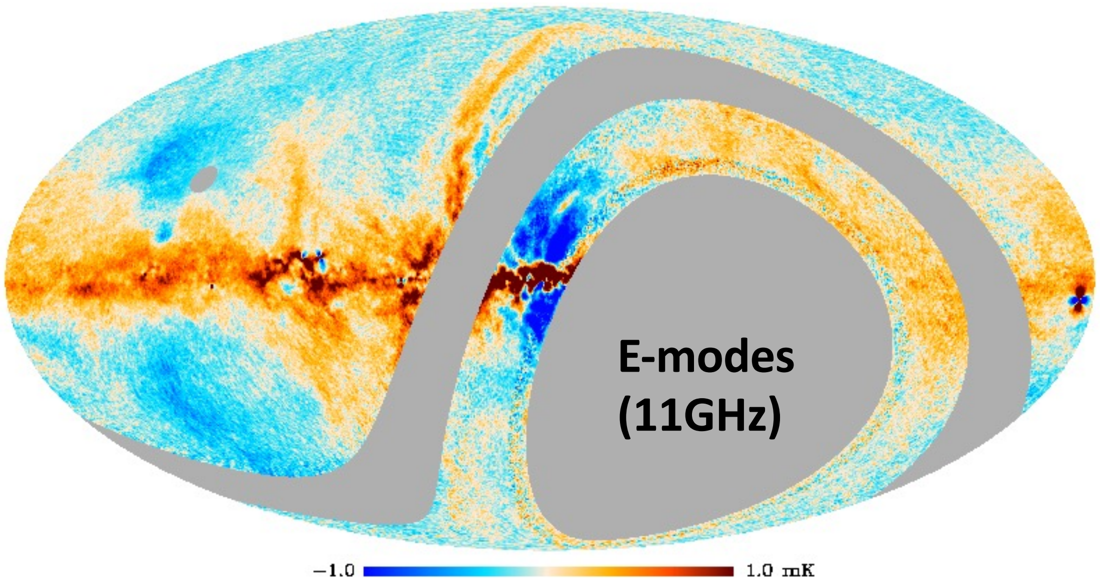

$$C_\ell^{XX} = A_{XX}\left(\frac{\ell}{80}\right)^{\alpha_{XX}} + c_{XX}$$

Mask	$\lvert b\rvert > 5°$	$\lvert b\rvert > 10°$	$\lvert b\rvert > 20°$
f_{sky}	0.38	0.34	0.27
	EE and BB fitted separately		
A_{EE} [μK^2]	1.52 ± 0.15	1.05 ± 0.18	0.81 ± 0.19
A_{BB} [μK^2]	0.52 ± 0.15	0.20 ± 0.12	0.18 ± 0.13
α_{EE}	−3.00 ± 0.16	−2.72 ± 0.26	−2.96 ± 0.36
α_{BB}	−3.08 ± 0.42	−3.13 ± 0.87	−3.12 ± 1.03
c_{EE} [μK^2]	0.07 ± 0.09	−0.13 ± 0.11	−0.09 ± 0.12
c_{BB} [μK^2]	0.10 ± 0.09	−0.06 ± 0.09	−0.09 ± 0.09
A_{BB}/A_{EE}	0.34 ± 0.10	0.19 ± 0.12	0.22 ± 0.18
	Joint EE and BB analysis		
A_{EE} [μK^2]	1.49 ± 0.12	0.97 ± 0.13	0.78 ± 0.14
α_{EE} (=α_{BB})	−3.04 ± 0.13	−2.83 ± 0.21	−3.03 ± 0.29
c_{EE} (=c_{BB}) [μK^2]	0.09 ± 0.06	−0.08 ± 0.06	−0.08 ± 0.07
A_{BB}/A_{EE}	0.36 ± 0.04	0.26 ± 0.07	0.26 ± 0.08

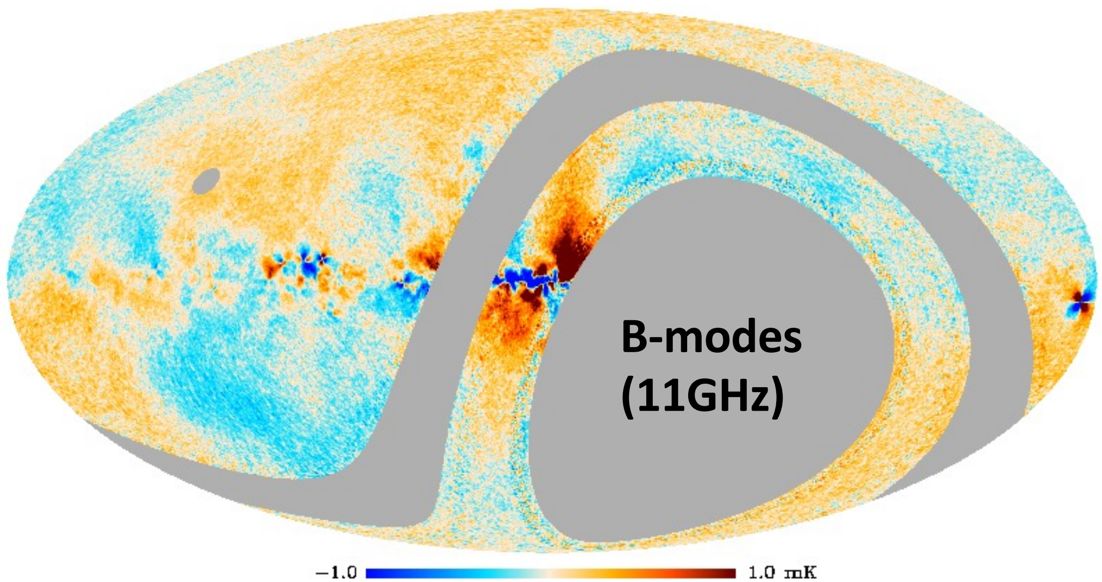

(Rubino-Martin et al. 2023)

Wide survey with the QUIJOTE MFI (10-20GHz)

Synchrotron E-B modes and E/B ratio

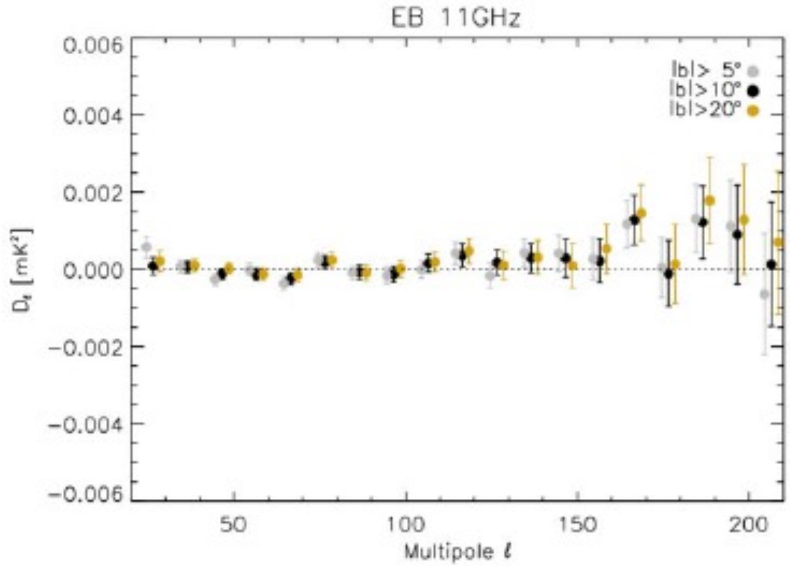

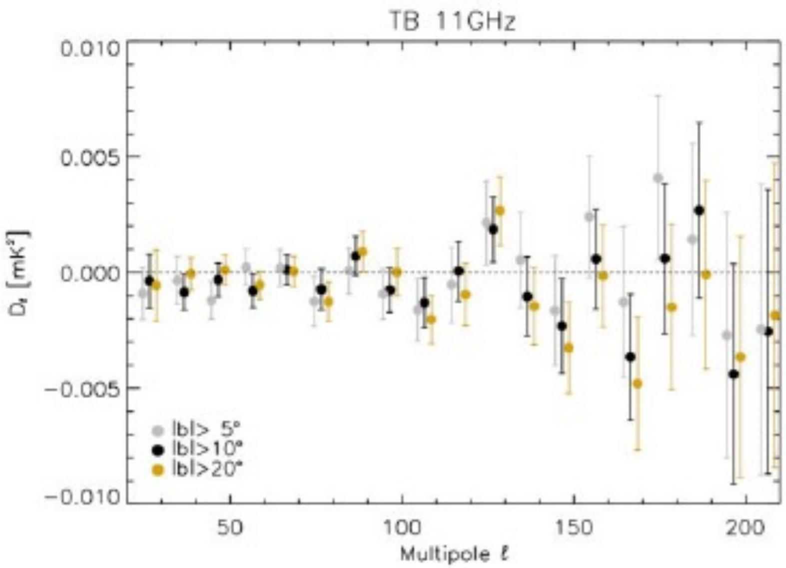

- Most prominent polarized structures (Fan, NPS, loops) appear in the E-map.
- **EE/BB ratio is approx. 4 at large scales**. Consistent with Martire et al. 2022 (WMAP+Planck).
- Analysis at power spectrum level confirms this result (Vansyngel et al. in prep.)
- For thermal dust, the ratio was closer to 2 (BB/EE~0.5, Planck Collaboration XI 2018).
- We measure **EB and TB consistent with zero**. Positive TE at large angular scales.

Mask	$\lvert b\rvert > 5^\circ$	$\lvert b\rvert > 10^\circ$	$\lvert b\rvert > 20^\circ$
A_{EB} [μK^2]	-0.014 ± 0.037	0.002 ± 0.038	0.043 ± 0.041
A_{EB}/A_{EE} ($\ell = 80$)	-0.010 ± 0.025	0.002 ± 0.038	0.057 ± 0.059
A_{TB} [μK^2]	-0.17 ± 0.24	-0.15 ± 0.20	-0.21 ± 0.19
A_{TB}/A_{EE} ($\ell = 80$)	-0.11 ± 0.16	-0.15 ± 0.20	-0.28 ± 0.28

$$C_\ell^{XX} = A_{XX}\left(\frac{\ell}{80}\right)^{\alpha_{XX}} + c_{XX}$$

(Rubino-Martin et al. 2023)

QUIJOTE-MFI wide survey results: synchrotron polarization

- Auto- and cross-spectra of QUIJOTE, WMAP, PLANCK maps in northern sky (|b|>10º).
- Dust-synchrotron correlation: ~ 0.18±0.06.
- Variability on sky (compared to other results: Planck Col. XI 2018, Krachmalnicoff et al. 2018).

Contamination of the CMB at 90 and 150GHz by the synchrotron B-modes. Regions at 95% C.L. :

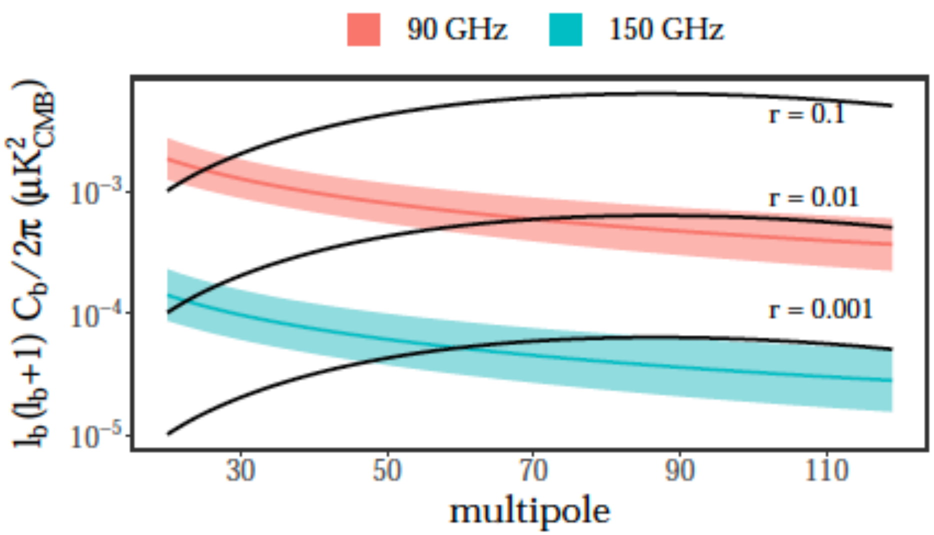

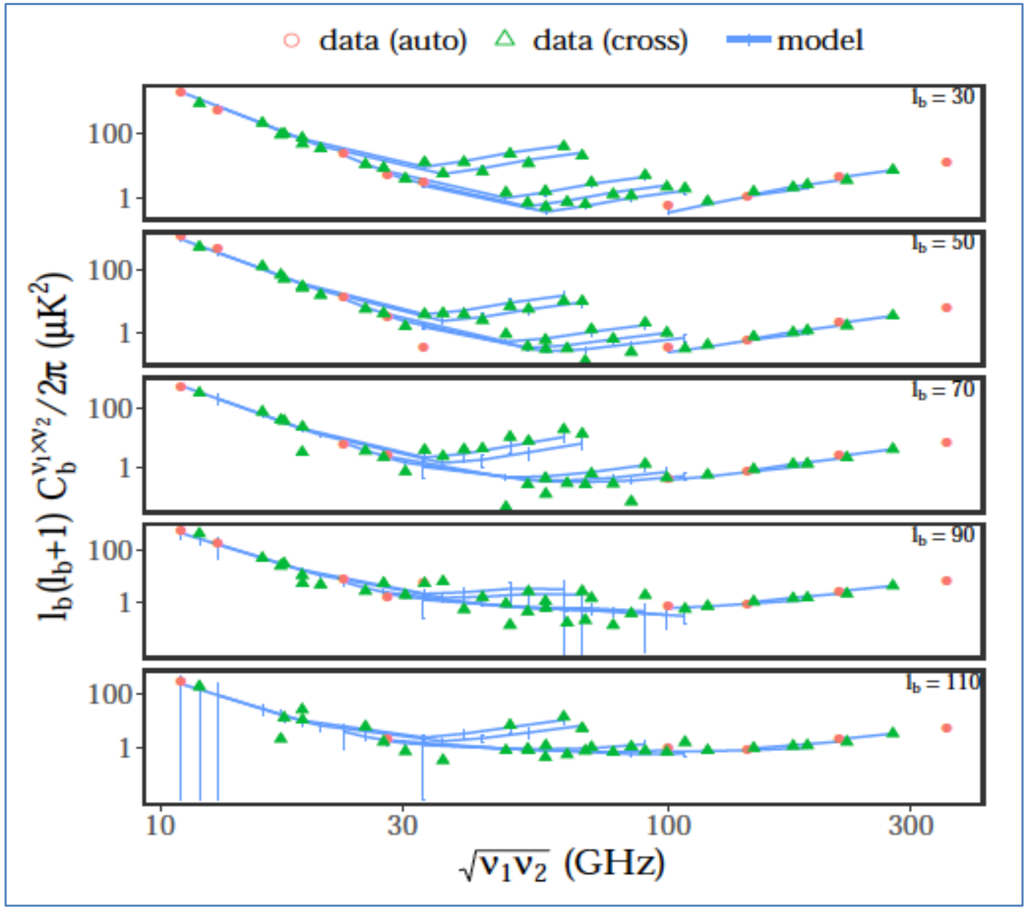

(Vansyngel et al. in prep)

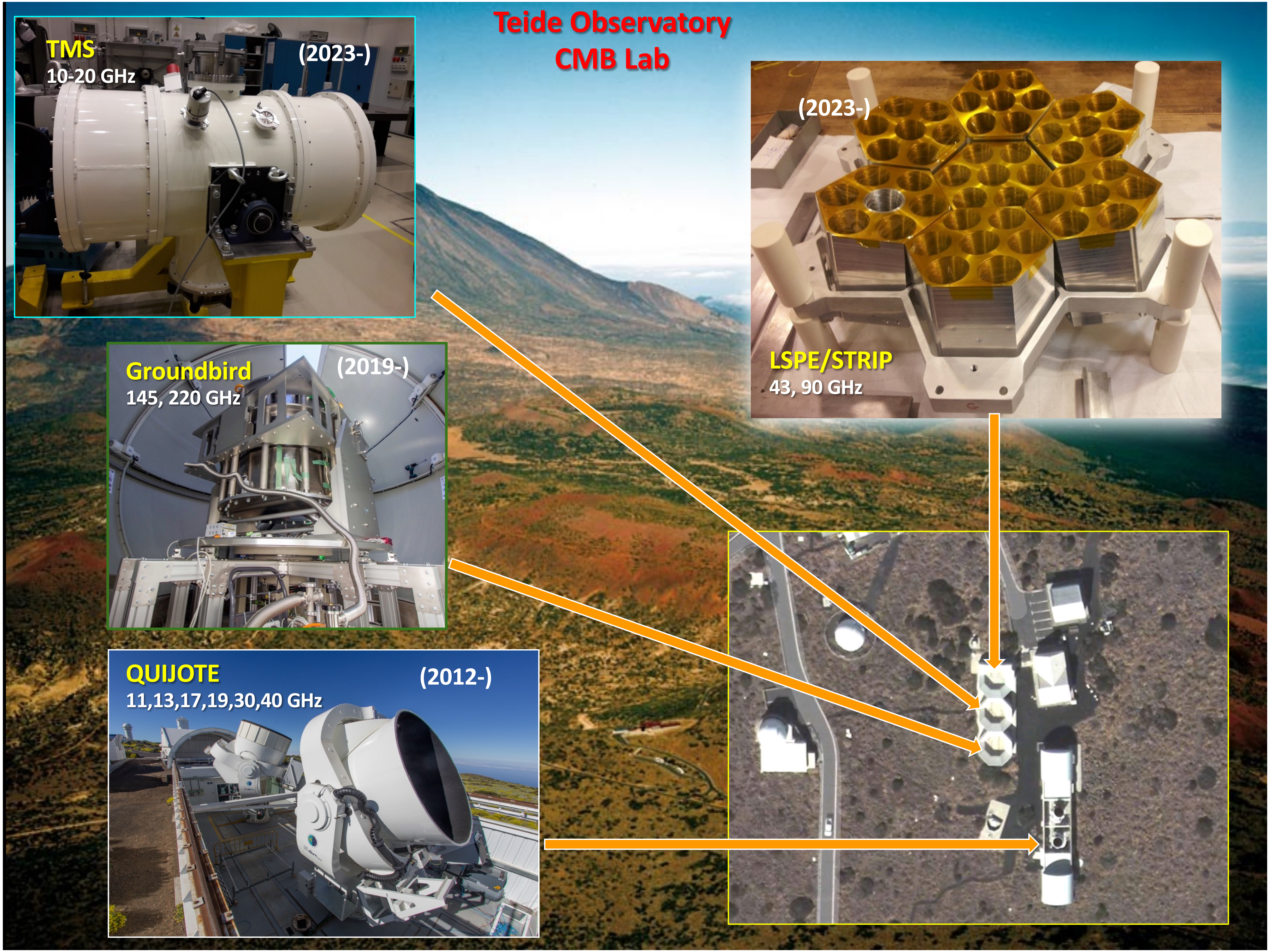
Teide Observatory
CMB Lab
TMS
10-20 GHz
(2023-)
(2023-)
LSPE/STRIP
43, 90 GHz
Groundbird
145, 220 GHz
(2019-)
QUIJOTE
11,13,17,19,30,40 GHz
(2012-)

Constraints on Primordial Magnetic Fields with Faraday Rotation. Impact of CMB foregrounds

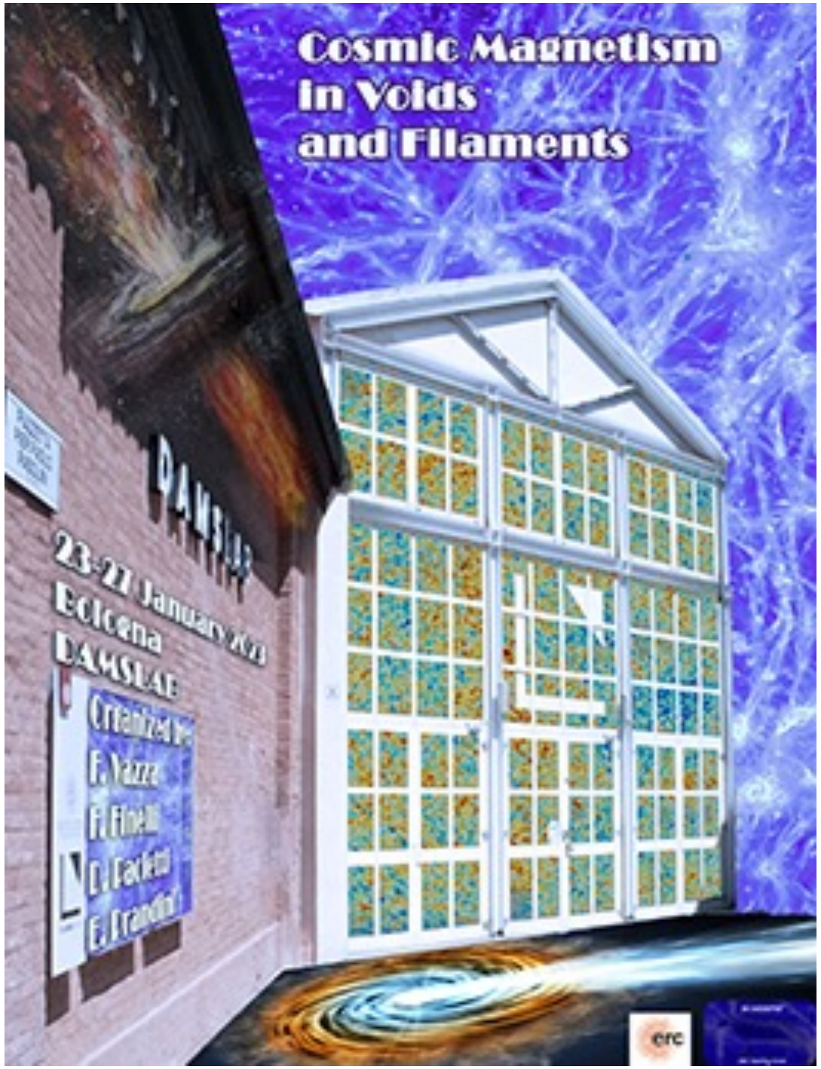

J.A. Rubiño- Martín (IAC)

Conclusions:

I. Faraday Rotation and PMFs.
   - Current limits at ~100nG for SI @1Mpc.
   - Room for improvement: Planck, Litebird, SO, CMB-S4.
   - Anisotropic biref. ~26nG for SI.

II. Impact of CMB foregrounds.
   - Galactic RM subdominant (<10 rad/m^2).
   - New low frequency data (SPASS, CBASS, QUIJOTE) provide an improved description of the polarized synchrotron (spatial variability of spectral index, TB consistent with zero, correlation with dust ~20%).

Thanks!

Extra slides

Tenerife Microwave Spectrometer (TMS), 10-20GHz

- **IAC project. Instrumental participation:**

- **Science driver**: Ground-based low resolution spectroscopy observations in the 10-20GHz range to characterize foregrounds (monopole signals; spectral dependence of monopole signals; ARCADE results) and CMB spectral distortions. Provides frequency intercalibration for QUIJOTE. (Rubino-Martin et al. 2020).
- **Location**: Teide Observatory (former VSA enclosure). Full sky dome.

- **Prototype for future instruments**. Also important **legacy value,** complementing future space missions.

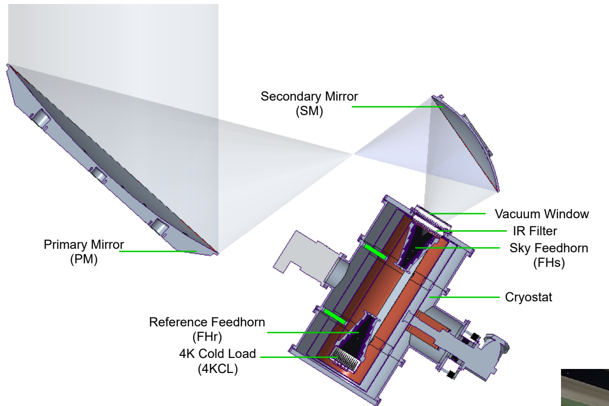

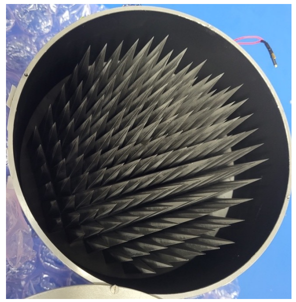

- **Proposed instrument concept**:
  - FEM cooled to 4-10K (HEMTs).
  - Reference 4K load.
  - DAS based on FPGAs.
  - ~3deg beam, 0.25 GHz spectral resolution (40 bands).

- **Project Status**:
  - Enclosure and dome at the Teide Observatory. ✓
  - Platform fabricated. Installation summer 2022. ✓
  - Mirrors designed (Alonso-Arias et al 2022). To be fabricated (→ Fall 2023).
  - Cryostat at the IAC since July 2019. ✓
  - Optomechanics in final fabrication phase.
  - Reference load fabricated (Nov 2021). ✓
  - DAS based on FPGAs (→ end 2023).
  - Commissioning in early 2024.

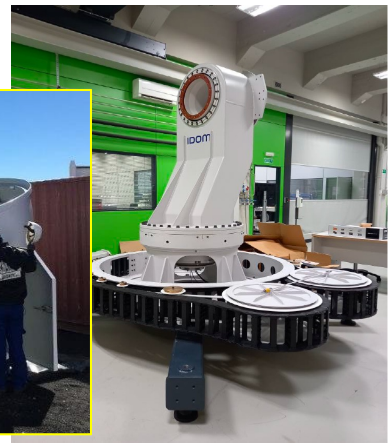

Ref. de la ayuda: ICTS-2019-03-IAC-12

Quijote
Q-U-I Joint Tenerife CMB experiment

MFI Instrument (10-20 GHz)

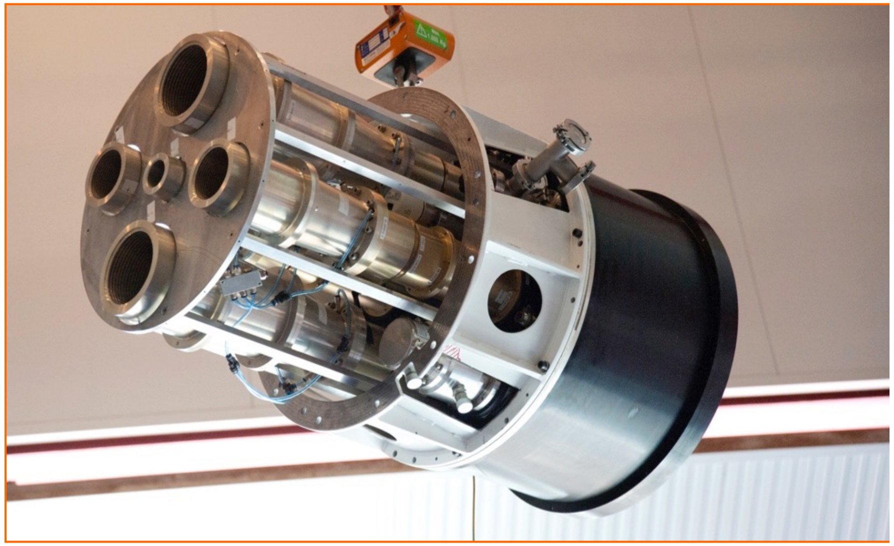

- **Operations**: Nov. 2012 – Dec. 2018.
- 4 horns, 32 channels. Covering 4 frequency bands: 11, 13, 17 and 19 GHz. Bandwidth 2 GHz.
- **Sensitivities**: ~700-800 μK $s^{1/2}$ in timelines.
- Near sidelobes ~ 35 dB, far-sidelobes < 80 dB
- f_{knee} ~ **250 mHz** (pol), ~**50 Hz** (int)
- "**HWP**": steeping polar modulator (RL<-20dB, IL< -0.15dB, I<-40 dB)

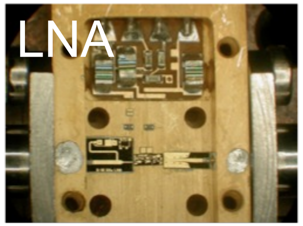

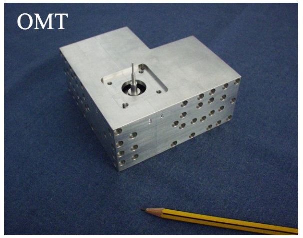

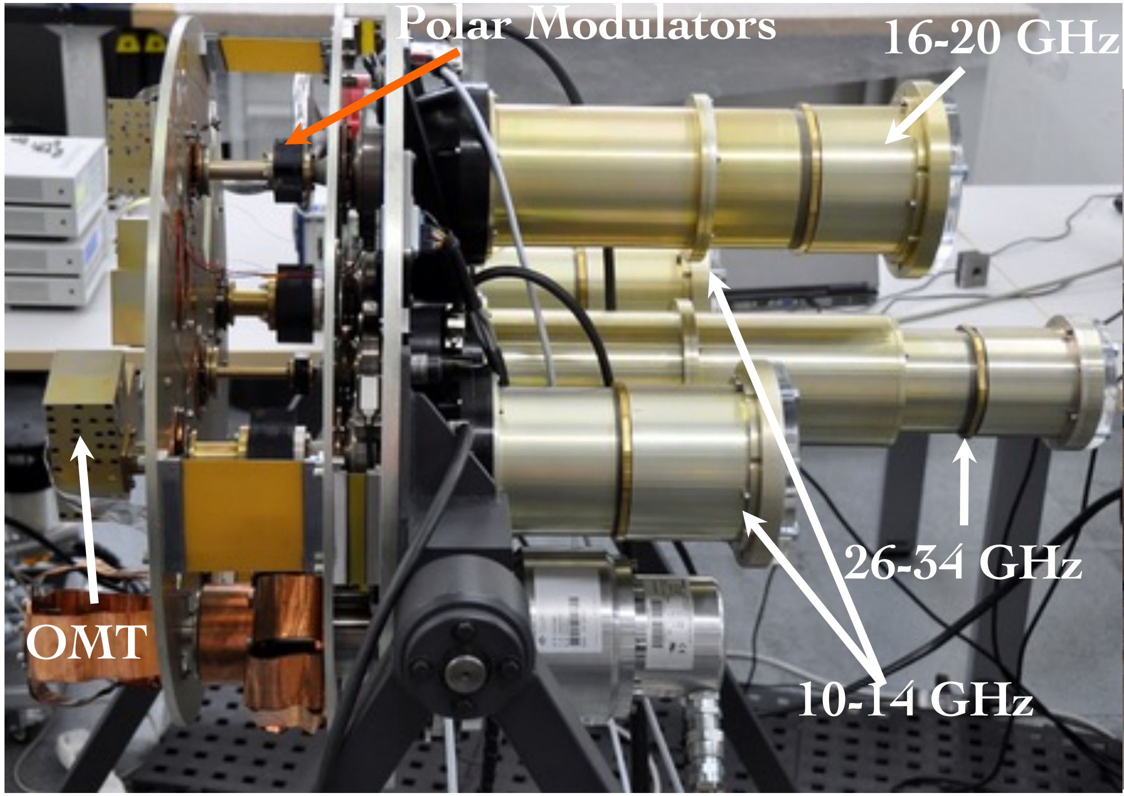

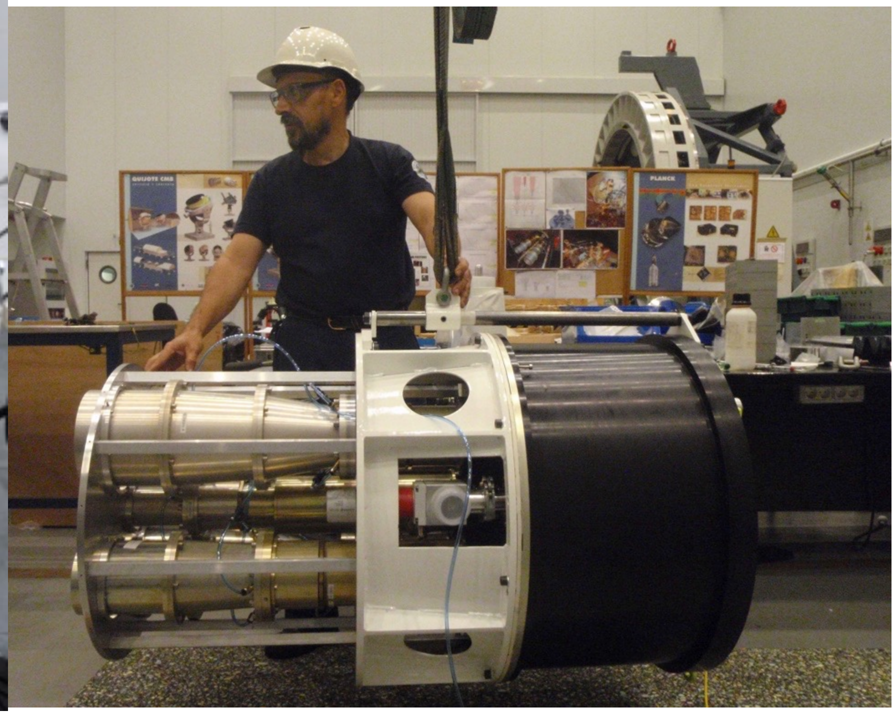

Science with QUIJOTE first instrument (MFI)

Excellent complement to PLANCK at low frequencies. Legacy for future experiments (→LiteBIRD)

MFI Science phase (Nov 2012- Dec 2018)

- Wide survey (10,800h) → RAW 10TB, binned TOD 340 GB.
- Cosmological fields (~3,000 deg^2) (6,500h)
- Daily calibrators (Crab, Cass A, Jupiter, sky dips,..) (1,700h)
- Galactic centre and Haze (1,400h)
- Perseus molecular cloud (750h) → Genova-Santos+15
- Fan region and 3C58 (500h)
- Taurus region (450h) → Poidevin+19
- SNRs (W44, W47, IC443, W63) (1,150h) → Genova-Santos+17
- M31 (540h)

Total: ~**26,000 h** of MFI data (3 effective years).
→ ~50% efficiency during science phase.

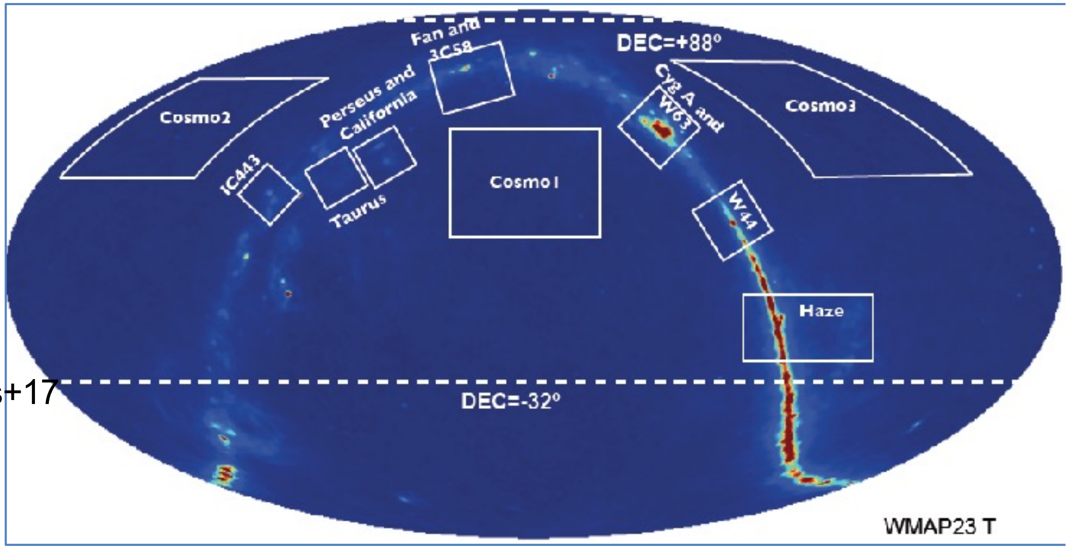

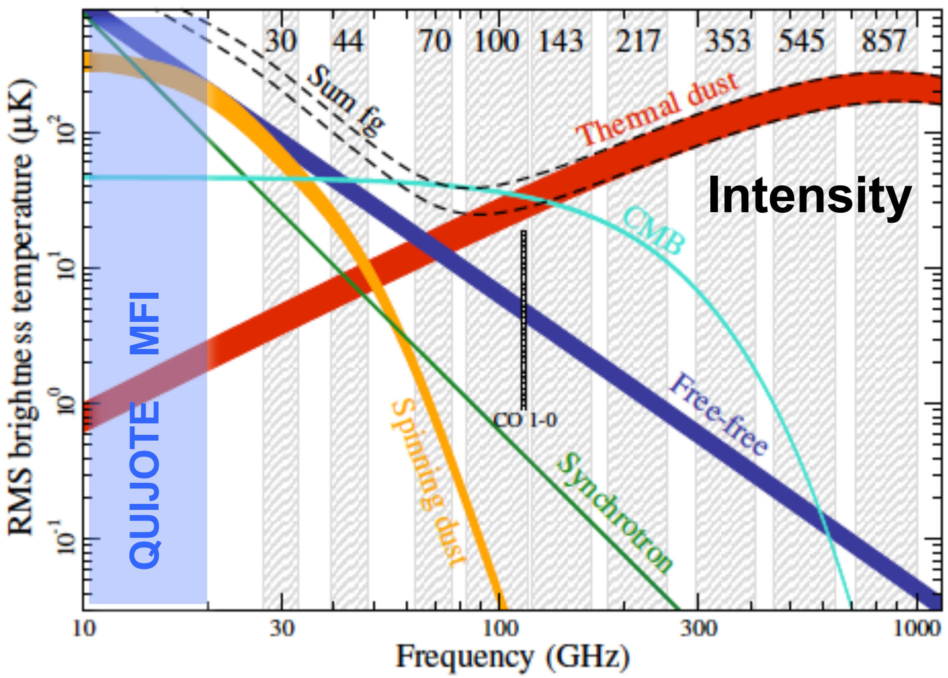

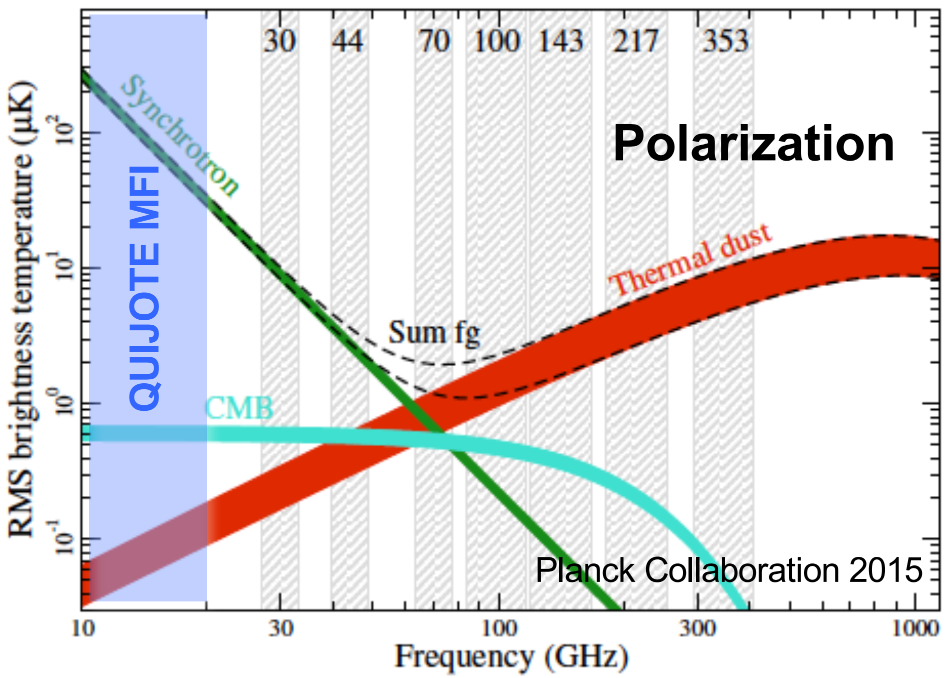

Wide survey with the QUIJOTE MFI (10-20GHz)

Noise properties of the maps

TT

EE

BB

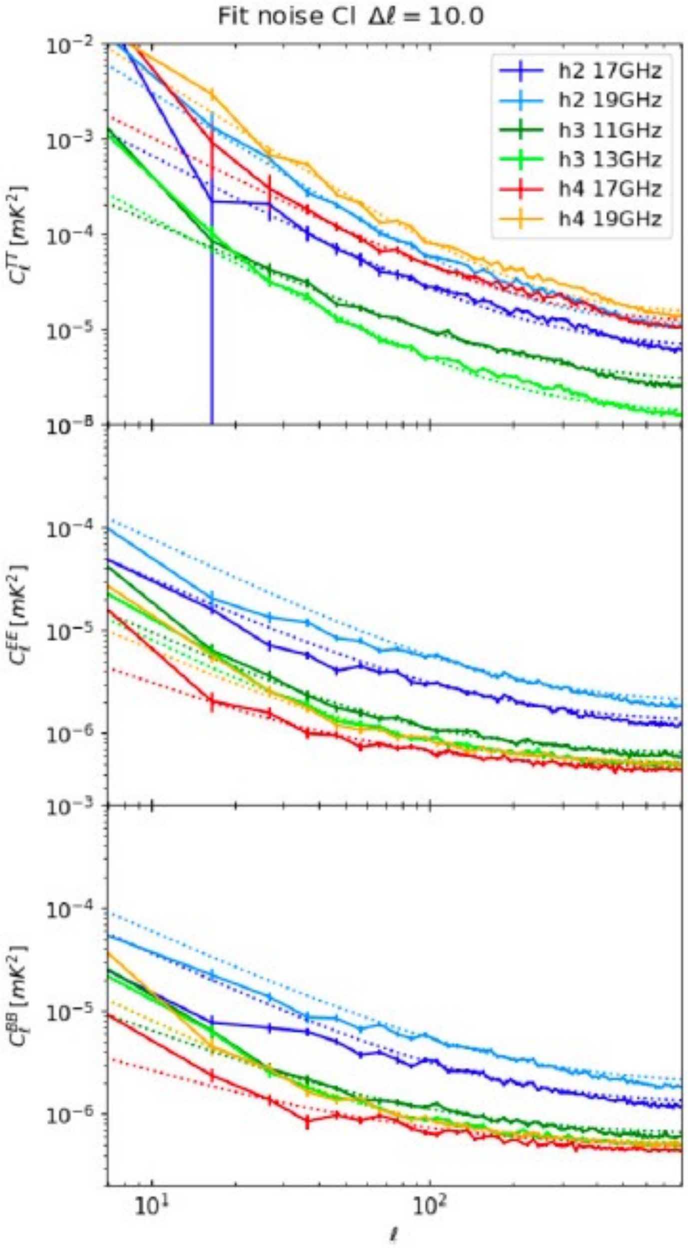

Channel [HFF]	C_w [mK^2 sr]	σ_{1° [μK]	α	ℓ_k
		Intensity (TT)		
217	6.13×10^{-6}	133.5	1.50	228.8
219	1.05×10^{-5}	174.5	1.82	229.3
311	2.56×10^{-6}	86.3	1.27	221.4
313	1.29×10^{-6}	61.3	1.60	192.5
417	1.07×10^{-5}	176.4	1.45	230.4
419	1.40×10^{-5}	201.7	1.82	243.6
		Polarization (EE)		
217	1.21×10^{-6}	59.4	1.20	145.0
219	1.87×10^{-6}	73.7	1.30	173.7
311	6.13×10^{-7}	42.2	1.24	86.0
313	4.95×10^{-7}	37.9	1.35	75.3
417	4.42×10^{-7}	35.8	1.06	53.5
419	5.02×10^{-7}	38.2	1.24	73.2

$$C_\ell = C_w \left(1 + \left(\frac{\ell_k}{\ell}\right)^\alpha\right)$$

- Noise correlations between frequencies of the same horn (H). E.g. ~80% between 11 and 13GHz in intensity, and ~33% in polarization.

(Rubino-Martin et al. in press)

Wide survey with the QUIJOTE MFI (10-20 GHz)

Final maps
(Smoothed to 1°)

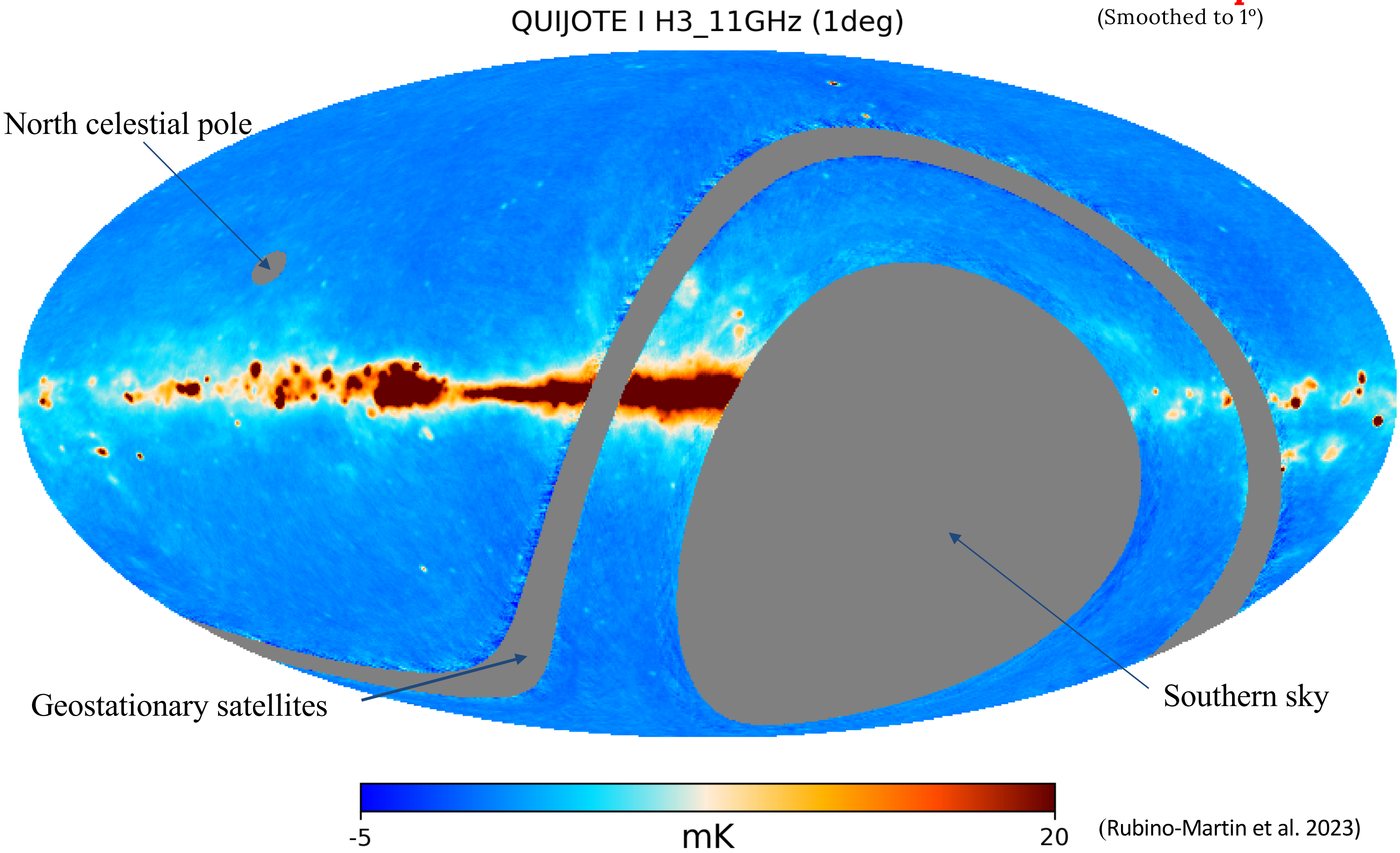

(Rubino-Martin et al. 2023)

Wide survey with the QUIJOTE MFI (10-20 GHz)

Final maps
(Smoothed to 1º)

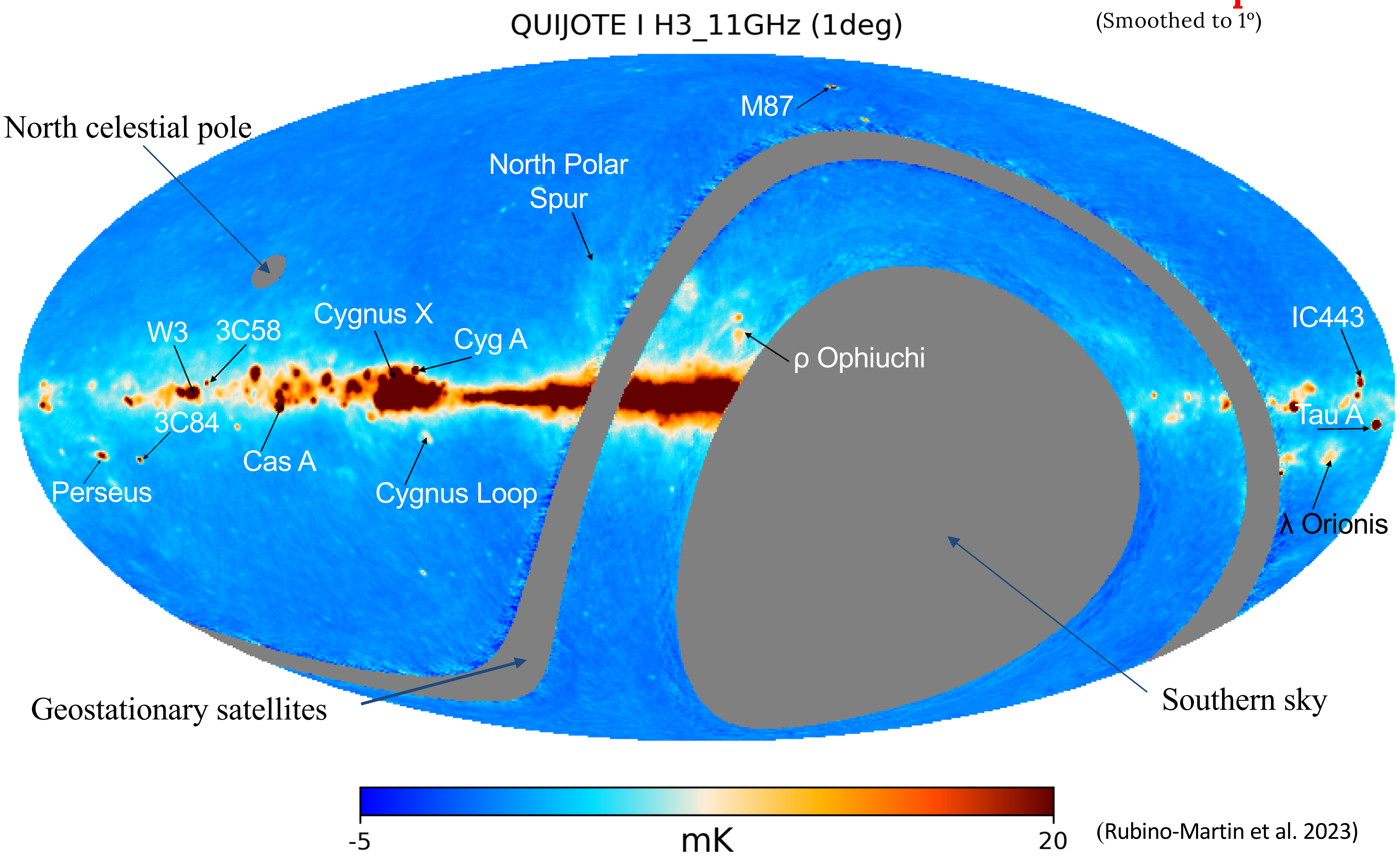

(Rubino-Martin et al. 2023)

Wide survey with the QUIJOTE MFI (10-20 GHz)

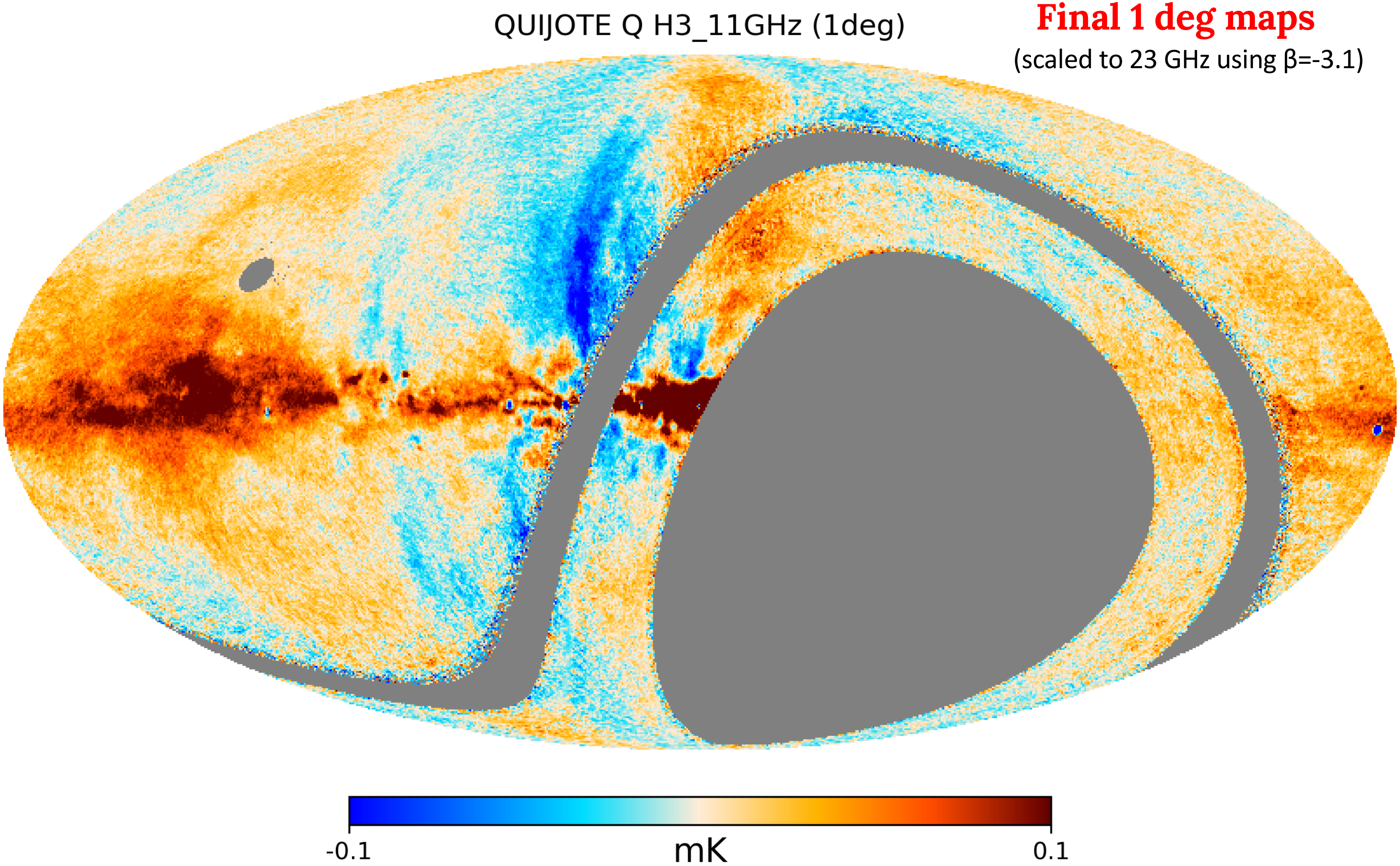

Final 1 deg maps

(scaled to 23 GHz using β=-3.1)

(Rubino-Martin et al. 2023)

Wide survey with the QUIJOTE MFI (10-20 GHz)

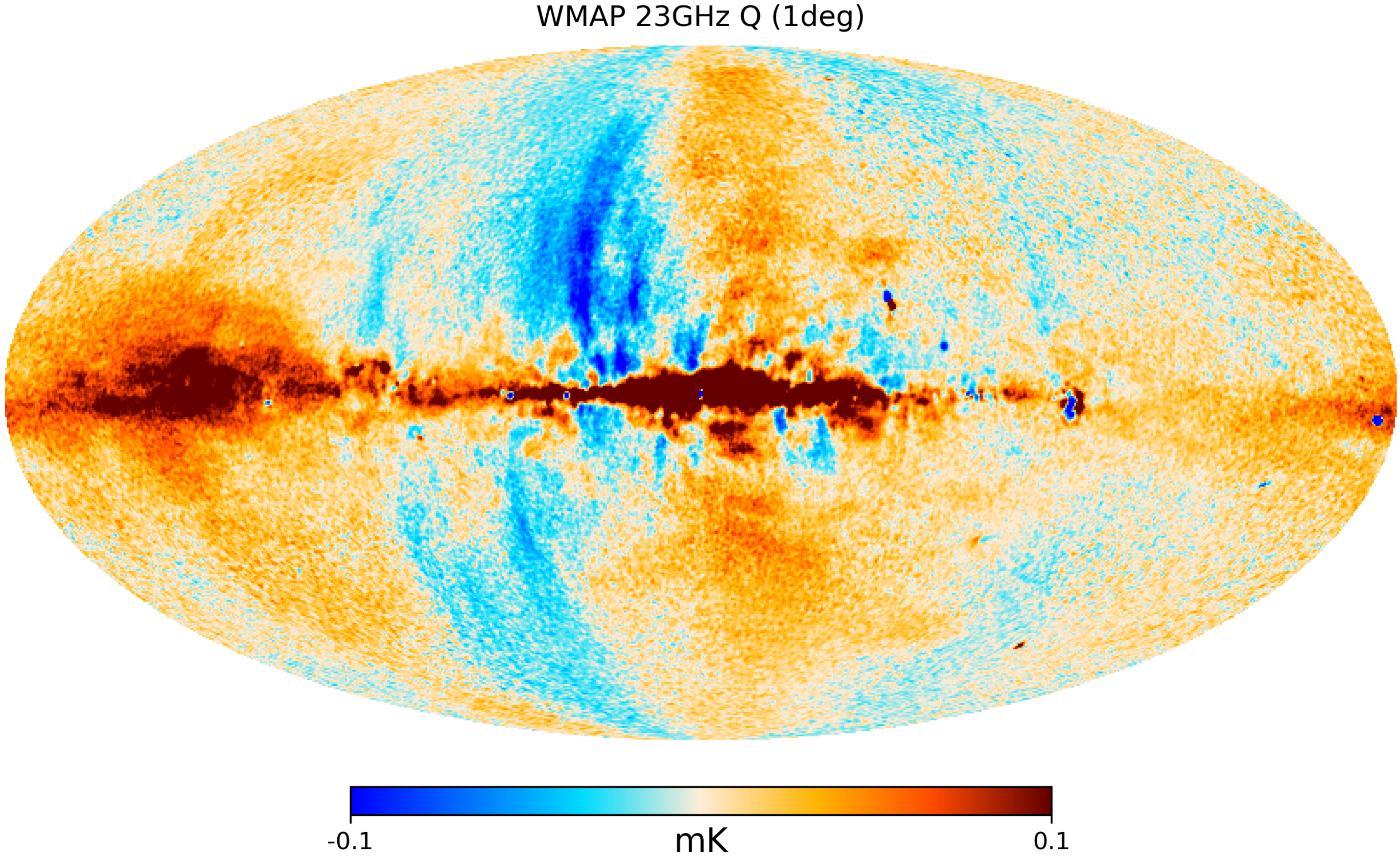

(Rubino-Martin et al. 2023)

Wide survey with the QUIJOTE MFI (10-20 GHz)

Final 1 deg maps

(scaled to 23 GHz using β=-3.1)

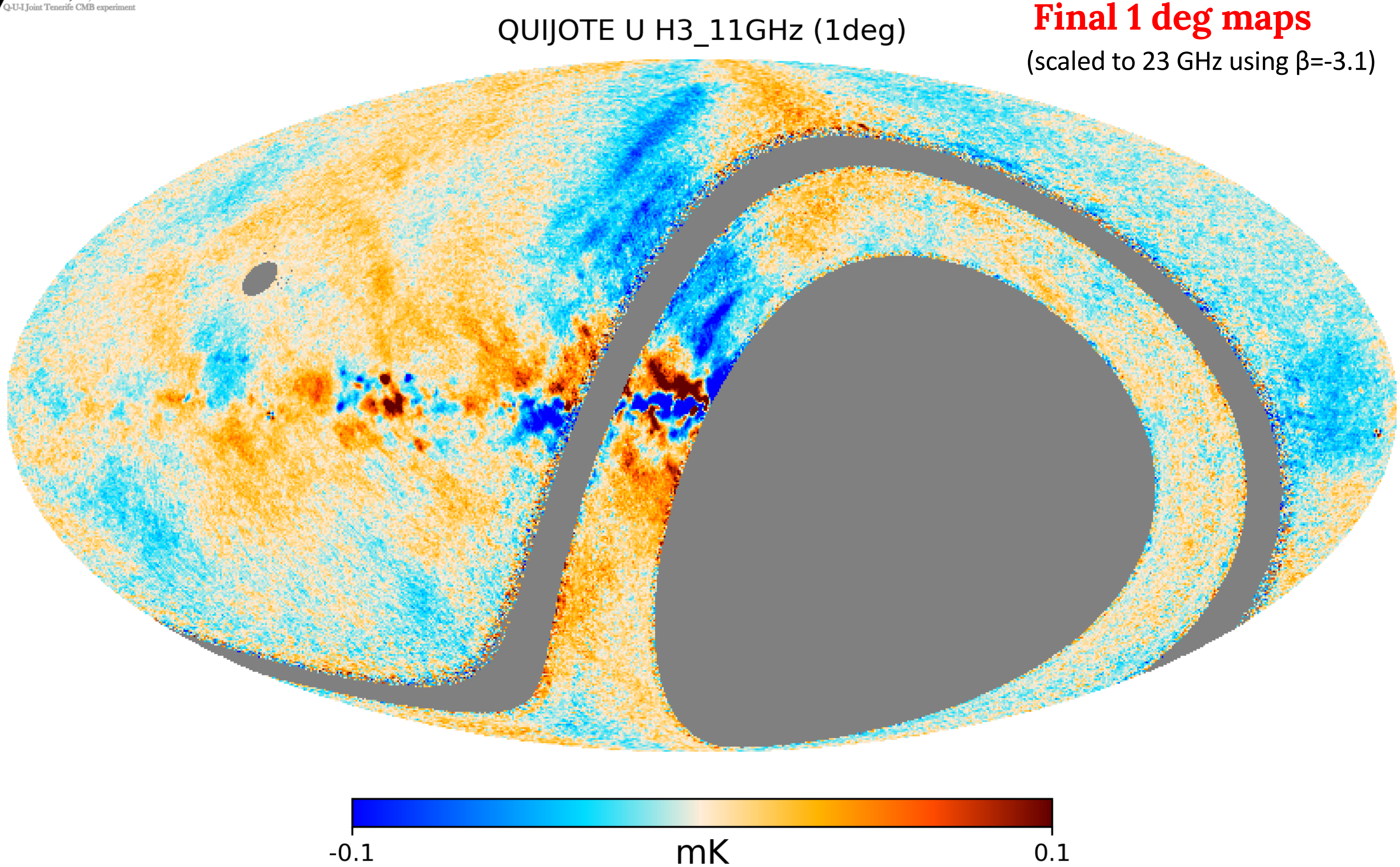

(Rubino-Martin et al. 2023)

Wide survey with the QUIJOTE MFI (10-20 GHz)

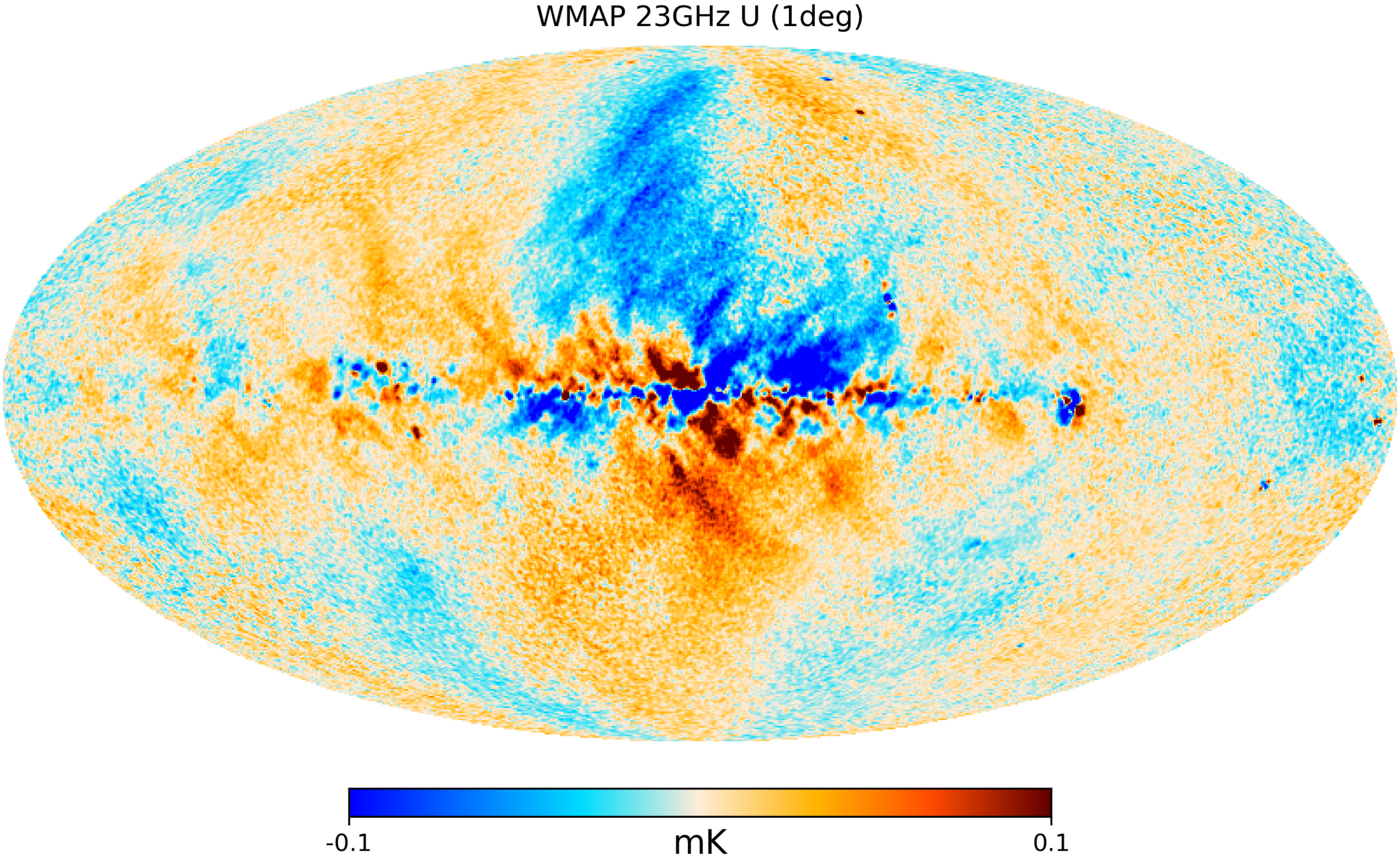

(Rubino-Martin et al. 2023)

Wide survey with the QUIJOTE MFI (10-20 GHz)

11GHz – 23GHz **13GHz – 23GHz**

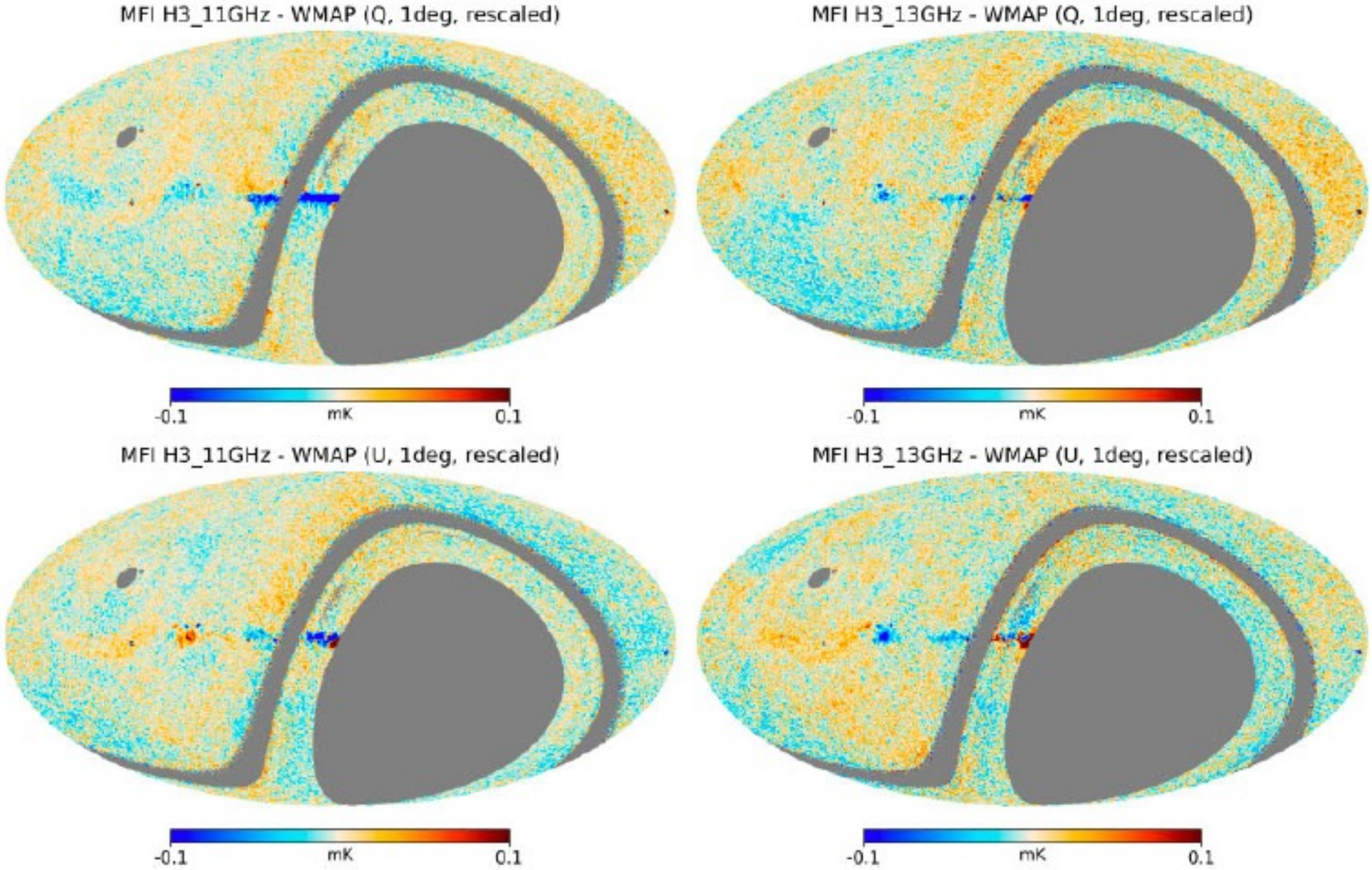

(Rubino-Martin et al. in press)

QUIJOTE-MFI wide survey results: modelling the AME

- **Génova-Santos et al. (2017):** Best upper limits on AME polarization to date , from W44 region (< 0.4% at 17GHz from QUIJOTE, and < 0.22% at 41GHz from WMAP).
- **Poidevin et al. (2023)**: Study of 56 compact AME sources (includes targets from PIR XV 2014).
- **Tramonte et al. (2023):** W49, W51 and IC443.
- **Intensity:**
  - QUIJOTE-MFI provides a cleaner separation of the AME, free-free and synchrotron components. Generally, higher AME and lower free-free. We find ν_{AME}= 23.6±3.6 GHz.
  - Clear correlation (90%) of AME/tau_{dust} with radiation field G_0. Seen in Tibbs et al. (2011, 2012), and PIR XV (2014).
  - Clear correlation between AME and dust peak. Poor correlation between G_0 and EM.

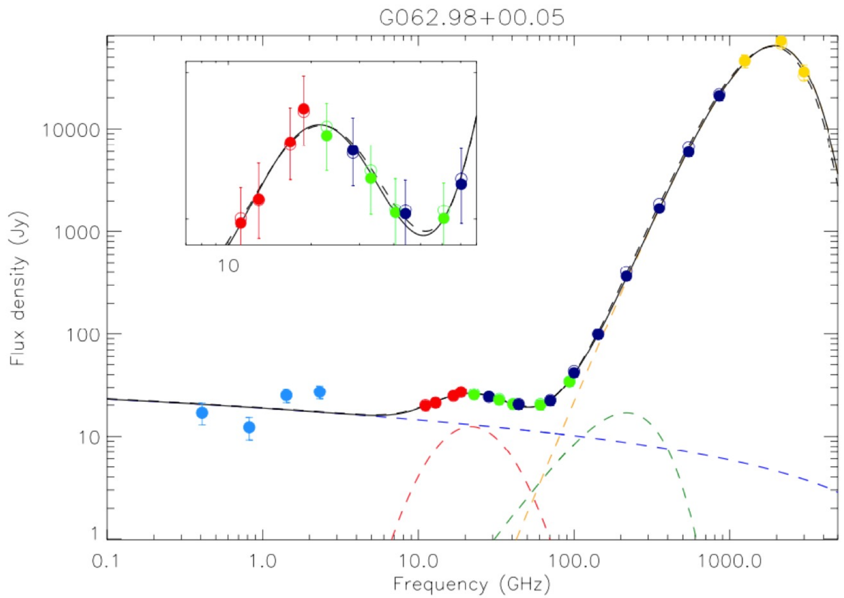

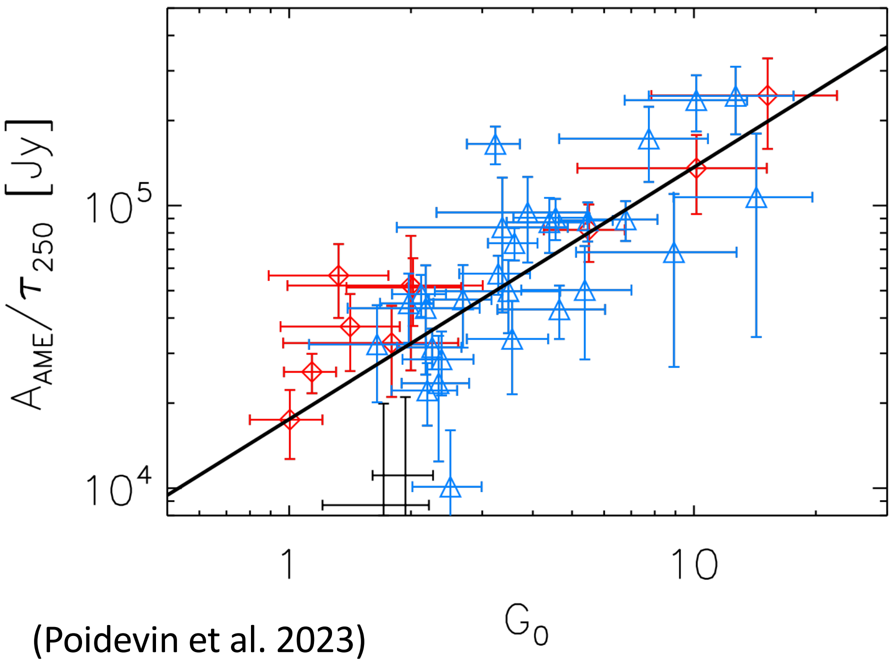

(Poidevin et al. 2023)

QUIJOTE-MFI wide survey results: the Haze emission

Data: wide-survey + raster scans

Intensity

- Haze component detected at 9σ, at 11 GHz. Confirmation of WMAP and Planck.
- Spectrum steeper (β=-2.79 ±0.08) than previous results (β=−2.56±0.05, Planck IX, 2013).

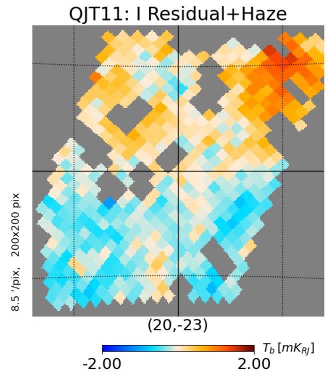

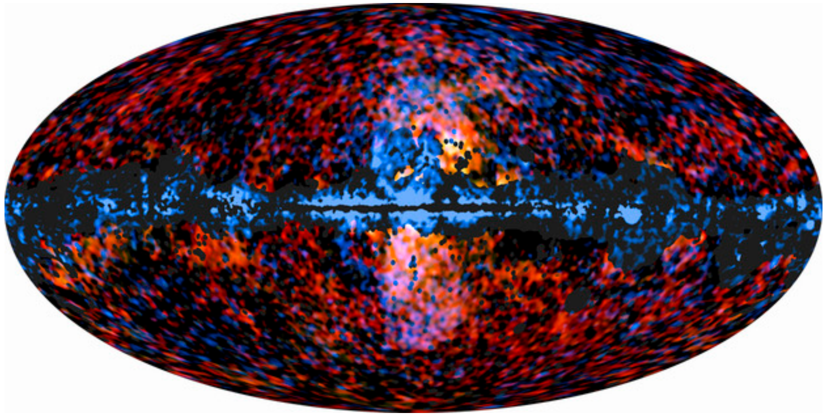

Planck (red) and Fermi (blue)

Polarization

- Sky signal residuals observed in polarization after subtracting other foregrounds: Haze? Possibly due to curvature of the synchrotron spectrum.
- TT-plots show flat spectra indices at 23-30 GHz and steep spectra at 11-23 GHz and 2.3-23 GHz.

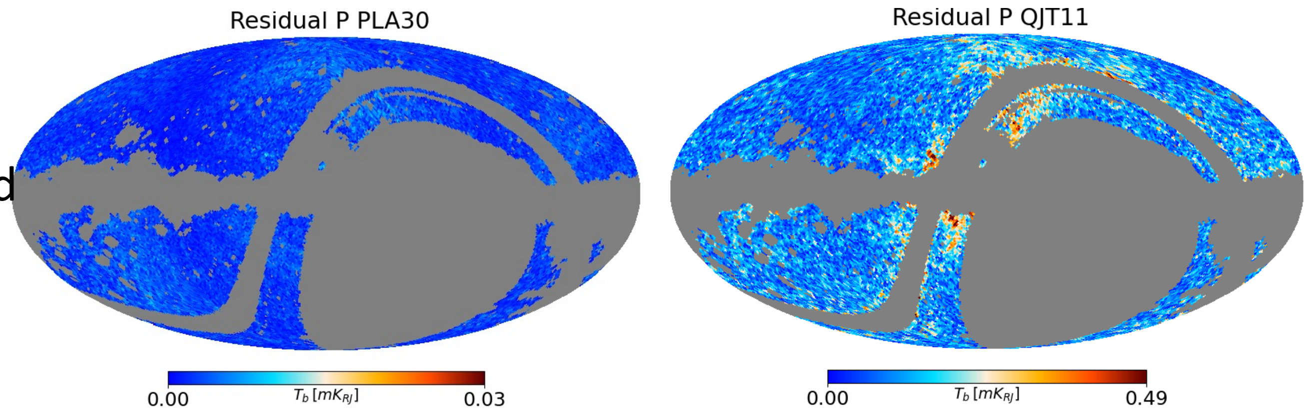

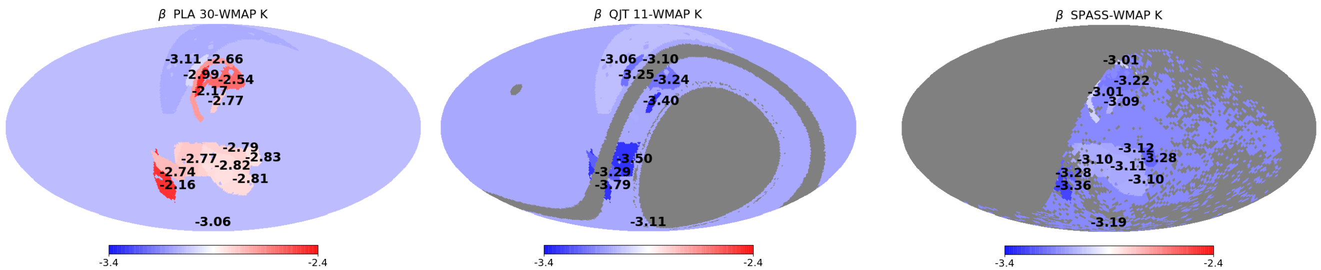

(Guidi et al. 2023)

MFI2 Instrument (10-20 GHz)

- **MFI upgrade (MFI2 @ QT-1)**. Fully funded. Aim: to increase the integration speed of the MFI by a factor 3 (mainly coming from the new LNAs) → Sensitivity of < 1μK.arcmin @ 100GHz (β=-3) in widey survey. Now 2.4μK.arcmin @100GHz.
- **5 horns**. Three covering the 10-14GHz band, and two covering 16-20GHz.
- Full digital back-end (FPGAs) → RFI removal.
- **Status**: Cryostat and opto-mechanical components fabricated & integrated. Now in verification phase.
- **Operations**: 3 effective years, starting early 2023.

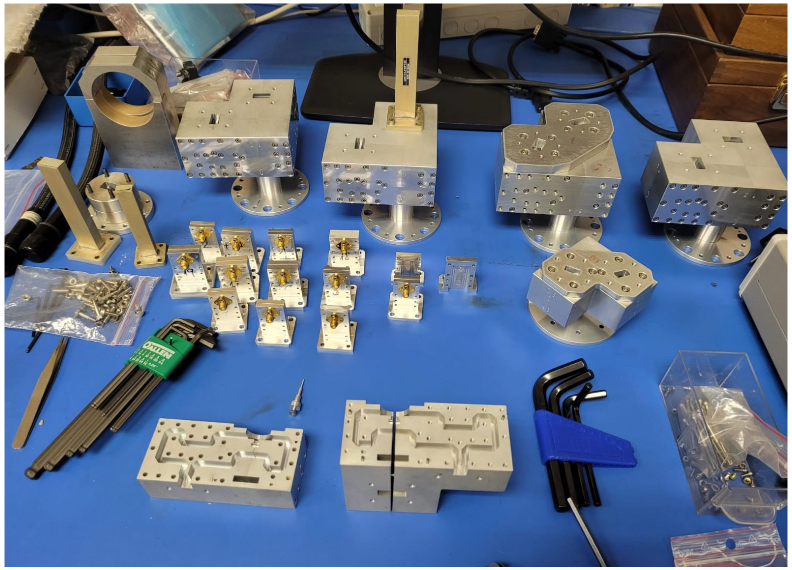

(Hoyland et al. 2022, SPIE)

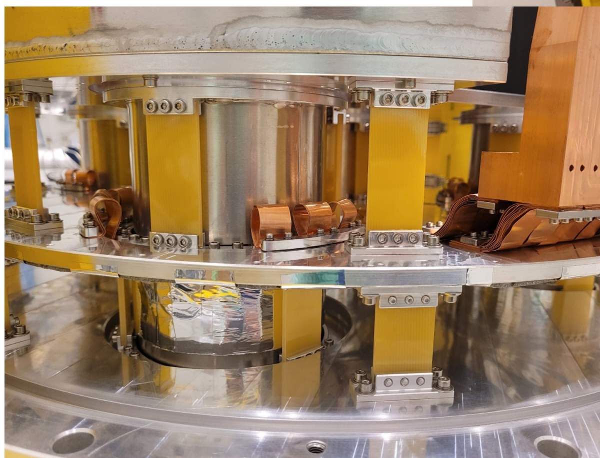

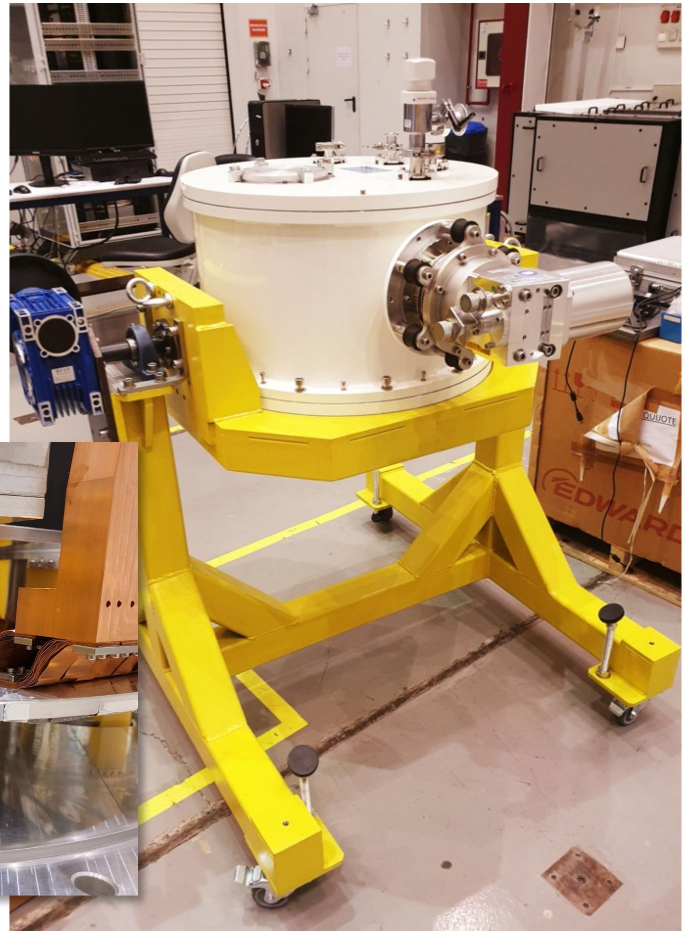

QUIJOTE-MFI wide survey results: accuracy of the calibration

Type of uncertainty	Applies to	11 GHz	13 GHz	17 GHz	19 GHz	Method
Calibration model	I,P	5 %	5 %	5 %	5 %	Model for calibrators
Colour corrections[a]	I,P	0.5 %	0.5 %	1 %	1 %	Bandpass measurements
Beam uncertainty	I,P	2 %	2 %	2 %	2 %	CST beam model, Tau A
Zero level [mK]	I	-0.74 ± 0.20	-0.59 ± 0.22	0	0	Plane-parallel model
I→P leakage	P	0.65 %	0.4 %	0.8 %	0.9 %	Cygnus area
Polarization efficiency	P	3 %	3 %	4 %	4 %	Lab measurements, Tau A
Polarization angle (deg)	P	0.6	0.9	1.0	3.2	Tau A, WMAP/Planck
Unknown systematics:						
Real space (μK/beam)	I	< 53	< 49	< 118	< 224	Null tests at $N_{\rm side} = 64$
Real space (μK/beam)	P	< 12	< 15	< 10	< 13	Null tests at $N_{\rm side} = 64$
Harmonic space ($30 < \ell < 200$)	I	0.2 %	0.3 %	0.5 %	0.7 %	Null tests
Harmonic ($30 < \ell < 200$)	P	3 %	4 %	6 %	6 %	Null tests
Overall calibration error[b]	I	5 %	5 %	5 %	5 %	
Overall calibration error[b]	P	5 %	5 %	6 %	6 %	

[a] These numbers should be multiplied by $|\alpha + 0.3|$, being α the spectral index of the source.

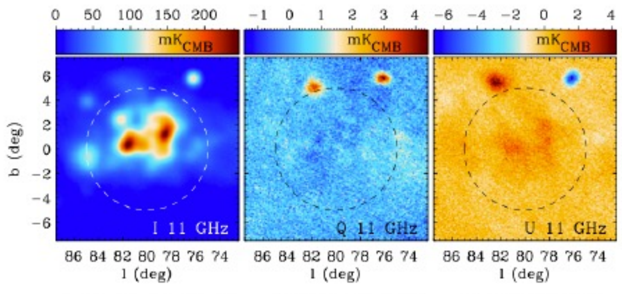

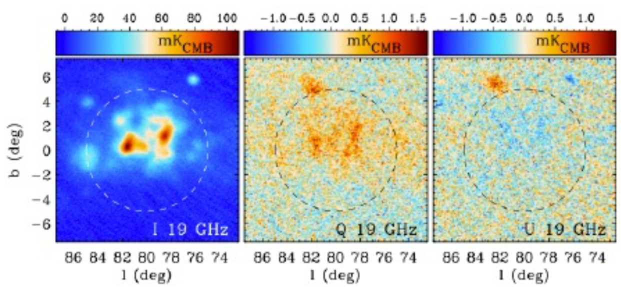

(Rubino-Martin et al. 2023)